applied system innovation

MDPI

Article

Design, Manufacturing, and Electroencephalography of the Chameleon-1 Helmet: Technological Innovation Applied for Diverse Neurological Therapies

Asaf J. Hernandez-Navarro [1], Gerardo Ortiz-Torres [1], Alan F. Pérez-Vidal [1], José-Antonio Cervantes [1], Felipe D. J. Sorcia-Vázquez [1], Sonia López [1], Moises Ramos-Martinez [1], R. E. Lozoya-Ponce [2], Néstor Fernando Delgadillo Jauregui [3], Jesse Y. Rumbo-Morales [1,*] and Reyna I. Rumbo-Morales [4]

[1] Computer Science and Engineering Department, University of Guadalajara, Ameca 46600, Mexico; asaf.hernandez5949@alumnos.udg.mx (A.J.H.-N.); gerardo.ortiztorres@academicos.udg.mx (G.O.-T.); alan.perez@academicos.udg.mx (A.F.P.-V.); antonio.alvarez@academicos.udg.mx (J.-A.C.); felipe.sorcia@academicos.udg.mx (F.D.J.S.-V.); sonia.lopez@academicos.udg.mx (S.L.); moises.ramos@valles.udg.mx (M.R.-M.)
[2] Tecnológico Nacional de México, Instituto Tecnológico de Chihuahua, División de Estudios de Posgrado e Investigación, Av. Tecnológico 2909, Chihuahua 31200, Mexico; ricardo.lp@chihuahua.tecnm.mx
[3] Natural and Exact Sciences Department, University of Guadalajara, Ameca 46600, Mexico
[4] Architecture and Design, Division of Arts and Humanities, Calzada Independencia Norte, University Center for Art, Huentitán El Bajo 44250, Mexico; reyna.rumbo7221@alumnos.udg.mx
* Correspondence: jesse.rumbo@academicos.udg.mx

Abstract: Brain activity plays a fundamental role in science and technology, particularly in the advancement of cognitive process therapies. Gaining a deeper understanding of brain function can contribute to the development of more effective therapeutic strategies aimed at enhancing cognitive performance and mental well-being. Advances in technological innovation in the health sector have allowed the creation of portable wireless electroencephalogram (EEG) devices, which make recordings in contexts outside the laboratory or clinical area. This work aims to design, manufacture, and acquire data on the Chameleon-1 helmet used by young and adult people people in different health states. The data acquisition of the EEG signals is carried out using two electrodes positioned at points F_3 and F_4, which are placed with the international 10–20 system. Tests were performed on several university participants. The recorded results show reliable, precise, and stable data in each patient with an average concentration of 91%. Excellent results were obtained from patients with different health conditions. In these records, the efficiency and robustness of the Chameleon-1 helmet were verified in adapting to any skull and with good data precision without noise alteration.

Keywords: brain disorders; EEG; helmet; Chameleon-1

check for updates

Academic Editors: Christos Douligeris and Wenbing Zhao

Received: 20 January 2025
Revised: 9 March 2025
Accepted: 3 April 2025
Published: 18 April 2025

Citation: Hernandez-Navarro, A.J.; Ortiz-Torres, G.; Pérez-Vidal, A.F.; Cervantes, J.-A.; Sorcia-Vázquez, F.D.J.; López, S.; Ramos-Martinez, M.; Lozoya-Ponce, R.E.; Jauregui, N.F.D.; Rumbo-Morales, J.Y.; et al. Design, Manufacturing, and Electroencephalography of the Chameleon-1 Helmet: Technological Innovation Applied for Diverse Neurological Therapies. *Appl. Syst. Innov.* **2025**, *8*, 56. https://doi.org/10.3390/asi8020056

Copyright: © 2025 by the authors. Published by MDPI on behalf of the International Institute of Knowledge Innovation and Invention. Licensee MDPI, Basel, Switzerland. This article is an open access article distributed under the terms and conditions of the Creative Commons Attribution (CC BY) license (https://creativecommons.org/licenses/by/4.0/).

1. Introduction

Advancements in health technology have had a significant impact and have led to scientific contributions, mainly through developments in electroencephalography (EEG) with dry or wet electrodes and new boards that can acquire data in real time via wireless connections [1]. These innovations have driven the creation of new EEG equipment to monitor the cognitive state, diagnostics, treatment, and therapies using new neuroelectro headbands. Neuroimaging techniques are used to reveal brain functions, behaviors, and emotions. One of these techniques was developed by [2], in which they present a high-resolution spatio-temporal photoacoustic neuroimaging technique (PANI) with a wide field

of view sufficient to cover the entire mouse brain cortex in the transverse plane and measure rapid neuronal dynamics. Likewise, other equipment has been developed based on a new type of OST-HMD optical system that includes three wedge-shaped free-form prisms and two symmetric lenses, which generates a result 50% higher than other OST-HMD optical solutions [3–5].

The EEG is a non-invasive neuroimaging technique that records the electrical activity generated by neuronal firing in the brain, offering high temporal resolution essential for understanding neural dynamics and cognitive processes [6,7]. EEG has played a crucial role in clinical diagnostics and research settings, enabling investigations into neurological disorders, brain–computer interfaces (BCIs), and cognitive neuroscience [8]. Traditional EEG systems are effective but have limitations such as cumbersome setups, the need for conductive gels, and lack of portability, which hinders their use in real-world applications and long-term monitoring [9]. Recent advances have concentrated on creating customized portable EEG headsets that improve user comfort and accessibility while maintaining signal quality [10,11].

In recent years, significant progress has been made in the design and manufacturing of EEG headsets, utilizing innovative materials and technologies to improve usability. For example, ref. [12] introduced a flexible ear EEG known as cEEGrid, which provides long-term discreet and comfortable EEG monitoring. The development of dry electrode technology has been a focal point, eliminating the need for conductive gels and reducing the setup time. Similarly, ref. [13] presented a wireless EEG headset using dry electrodes and flexible printed circuit boards, improving user comfort and mobility. The importance of standardizing metrics for the evaluation of new EEG technologies in real-world settings was highlighted by [14]. This standardization is crucial to ensure consistent performance evaluation across various EEG devices. They proposed a framework for benchmarking the performance of new EEG devices, highlighting factors such as signal quality, user comfort, and ease of use. Their work provides guidelines for evaluating and comparing emerging EEG technologies to ensure reliability and validity in practical applications [15,16].

Different studies have shown the potential offered by brain–computer interfaces (BCI)-based systems to be used as part of nonpharmacological treatments in people living with ADHD [17]. In such cases, Plan-It Commander is a BCI video game designed to promote the learning of cognitive skills among children with ADHD [18]. Harvest Challenge is a 3D virtual reality video game designed to train attention self-regulation in children with ADHD using a BCI system [19]. Focus Pocus is a themed training video game that is used in cognitive training therapies to reduce the symptoms of ADHD [20]. FarmerKeeper is a video game based on a BCI system designed to improve the attention of children with autism and ADHD [21]. CogniDron-EEG is a system based on a BCI for flying a drone indoors for cognitive training purposes [22].

The evolution of 3D printing technology has opened new doors for the rapid prototyping and customization of EEG headsets. The ninjaCap, a 3D printed headgear explicitly designed for functional Near Infrared Spectroscopy (fNIRS) and electroencephalography applications, was introduced by [23]. The ninjaCap offers a precise method for probe placement, using atlas-based or subject-specific head models and an innovative spring-relaxation algorithm to flatten 3D brain coordinates onto 2D printable panels. This approach improves sensor accuracy, reduces labor-intensive manual processes, and improves both comfort and signal quality, making it suitable for various research and clinical applications. A novel 3D-printed, directly conductive, and flexible EEG electrode system was presented in [24]. This system eliminates the need for Silver/Silver-Chloride (Ag/AgCl) coatings, significantly reducing manufacturing time and costs. The flexible electrodes are flexible to different head shapes and do not require conductive gels, making them more user-friendly in real-world

applications. Despite the challenges posed by higher contact impedance and increased noise sensitivity, these electrodes offer promising advancements for low-cost personalized EEG systems, particularly in BCI applications [25].

In [26], an ergonomic EEG headset is developed using 3D anthropometry to improve fit and usability. Traditional EEG caps face challenges with comfort, proper electrode placement, and usability in real world environments. Using statistical shape modeling, the authors designed a one-size-fits-all BCI headset that accommodates human head shape and size variations. This approach promises to improve the stability and repeatability of electrode placement, offering a more user-friendly solution than current commercial headsets, which often suffer from poor fit and inconsistent signal quality [27].

The quality of electroencephalography (EEG) signals is essential both in clinical applications and in research. One of the most important factors influencing the quality of these signals is the design of the EEG helmet, especially regarding proper fit and the flexibility of the sensors. A well-designed helmet that ensures a good fit and proper electrode placement significantly improves the accuracy of the obtained signals. For example, the article [28] examines the latest research on ergonomic aspects in brain–computer interfaces (BCIs). It addresses dry electrodes, which allow the detection of brain signals with sufficient quality for BCI applications, analyzing their pros, cons, and performance. Additionally, a summary of the most recent efforts to create new interface designs that reduce fatigue and discomfort during prolonged and daily use is provided.

Proper EEG signal acquisition is crucial for improving neurological therapies, such as neurorehabilitation in patients with brain damage, controlling devices through brain–computer interfaces (BCIs), and diagnosing disorders like epilepsy [29] or insomnia [30]. A well-designed helmet facilitates the collection of accurate signals, contributing to the effectiveness of therapies.

In research, non-invasive EEG electrodes are key in neuroscience, brain–computer interfaces, and cognitive assessment, where a precise and stable signal is essential for studying cognition and brain mapping [31].

In the study by Hermann et al. [32], dry and wet electrodes were compared in EEG with 16 healthy subjects and 16 neurological patients. The results showed that although dry electrodes had slightly more artifacts and higher impedance, EEG signals, including evoked potentials, were comparable between both systems. Most participants preferred the dry electrodes for their ease of use and portability. These results suggest that dry electrodes are a viable option for both clinical and home applications with less susceptibility to electromagnetic interference.

In summary, the quality of EEG signals is crucial for the diagnosis and treatment of various neurological conditions, as well as for research in neuroscience, where different types of brainwaves provide valuable information about the state and function of the brain. Improving the design and fit of EEG helmets is essential to ensure the accuracy of these signals and optimize both therapies and scientific studies.

The work presented in [33] describes the design and development of an affordable portable EEG headset based on the OpenBCI Ultracortex Mark IV system. The primary goal is to improve the accessibility and usability of BCI technologies by providing a cost-effective and efficient solution for rehabilitation and remote control applications. The headset was validated through experiments with 20 participants and compared to commercial devices in terms of cost, signal quality, setup time, and comfort. The results showed that the self-designed device offers competitive performance, reduced setup time, and 82% precision in specific tasks, such as slide control through voluntary blinking. The authors conclude that this device presents a viable alternative for users with clinical and personal needs with potential for future design improvements and expanded applications.

The article presented by [34] focuses on the design of wearable EEG devices specialized for passive brain–computer interface (PBCI) applications. It addresses the challenge of optimizing electrode configurations to enhance the accuracy of detecting emotional and attentional states. Using EEG data sets related to emotion recognition and attention monitoring, the authors developed electrode setups specific to emotion, specific to attention, and general purpose, evaluating them in multiple configurations with two, four, six, and eight electrodes. Their results showed that optimized configurations outperformed conventional commercial devices, suggesting that specialized electrode placement can significantly improve the performance of PBCI systems. This research highlights the potential of customized EEG devices for various real-world applications, such as neurofeedback, consumer behavior analysis, and driver vigilance detection.

Unlike studies reviewed in the literature, this work presents an innovative EEG headband that allows precise sensor position adjustment and customization of the overall dimensions of the device, ensuring better fit and performance. The contributions of our work are as follows:

- Modular and adaptable design: the headband is compatible with various skull sizes, implementing an ergonomically optimized design, obtaining an improved arrangement of the electrodes that allows obtaining a more precise and focused signal in the region of interest that maintains optimal contact regardless of head shape.
- Optimized placement: The system positions all electronic components at the back of the head, minimizing external disturbances during EEG recordings.
- Use of advanced flexible materials: the headband incorporates polymer–conductor materials, ensuring precise sensor positioning, flexibility.

These features make this headband a highly versatile tool suitable for clinical and personal use, significantly improving existing devices.

This study aims to evaluate the quality, precision, and firmness of electrode placement in the Chameleon-1 helmet, comparing it with other EEG helmets and the standards of the 10–20 system. Additionally, it examines how a more precise and stable placement in positions F3 and F4, ensured by the helmet's secure fit on the head, influences the quality and stability of the EEG signal, as well as its effectiveness in measuring brain activity related to attention, concentration, and relaxation.

The specific objectives of this research are outlined below:

- To assess the quality, precision, and firmness of electrode placement in the Chameleon-1 helmet in comparison to other EEG helmets and the standards of the extended 10–20 system.
- To analyze the impact of more precise and firm electrode placement in F3 and F4, ensured by the helmet's secure fit, on the quality and stability of the EEG signal.
- To compare the performance of the Chameleon-1 helmet with other EEG helmets in measuring brain activity related to attention, concentration, and relaxation.

Based on these objectives, the hypothesis proposes that a more precise and stable placement of electrodes with the Chameleon-1 helmet, which minimizes movement due to the helmet's secure fit, enhances the quality and stability of the EEG signal in positions F3 and F4 compared to other EEG helmets. This improvement leads to a more reliable assessment of brain activity.

Although this study focuses on positions F3 and F4, the Chameleon-1 helmet allows for electrode placement in a broader range of positions within the extended 10–20 system, which may be considered in future research.

Its design and construction focused on its technological development and innovation, highlighting improvements in electrode placement accuracy and signal quality. Since the

helmet targets F3 and F4 and the surrounding electrodes, it could be useful in certain therapies. However, this study only evaluates its technological performance, not its therapeutic effects. For example, the results demonstrated that the proposed helmet allows for better detection of the subject's active and relaxed states compared to other helmets, which could be useful in applications such as neurofeedback, cognitive training, and stress monitoring.

This work is divided into the following sections. Section 2 shows the complete design of the innovative Chameleon-1 helmet, which has adaptability and precision at the measurement points for different skull dimensions. Section 3 presents the characteristics of the Chameleon-1 helmet, which is configured based on the international 10–20 system and uses mechanisms and electronics to perform precise sensing and acquire data without noise. Section 4 presents the results and discussion of the study conducted on multiple patients with different skull dimensions and brain signal readings.

2. Chameleon-1 Helmet Design (Neuro-Electro)

Based on the literature review, the design of this innovative technology focused on the health area has great scientific and technological contributions. The design of the Chameleon-1 helmet is compatible with most skull sizes, since it can be sized to different lengths and allows mobility on all its electrodes without affecting the signal acquired by the sensors. Most helmets found in the literature are limited in size and have poor ergonomics, and the electrodes remain fixed in one position. Likewise, certain devices developed have electrodes and an electronic card near the patient's forehead, and this can cause interference in the acquired signals. The design of the Chameleon-1 helmet has all the electronics located at the back of the head to reduce possible interference in the EGG signals and to obtain a better result in the reading and storage of electrical signals from the brain.

The Chameleon-1 helmet not only optimizes ergonomics and reduces interference but also incorporates materials that allow for precise flexibility and fit, adapting to various head shapes without compromising measurement quality. These materials include flexible conductive polymers that ensure the implementation of an ergonomically optimized design and an improved arrangement of the electrodes that allows obtaining a more precise and focused signal in the region of interest. The modular design of the headband, coupled with its mobility, enables the flexible integration of different sensor types, allowing for precise positioning and adjustment.

One of the most innovative features of the Chameleon-1 helmet is its precise positioning of each electrode, allowing for real-time monitoring with accurate performance at measurement points based on the 10–20 system. This facilitates its use in non-laboratory environments, such as in field studies or at home, allowing patients or research participants to maintain their mobility and daily routine without interruption. The international 10–20 system is an internationally recognized method for describing the location of each electrode. The numbers 10–20 refer to the percentage (10 and 20) of distance at which the electrodes should be placed on the frontal, occipital, right, and left sides of the skull, as can be seen in Figure 1.

One of the promising applications of the Chameleon-1 helmet is its ability to capture high-quality signals without the need for extensive patient preparation, making it an ideal tool for continuous therapies or prolonged sessions, such as the treatment of neurological therapies. Likewise, its portability, user-friendly design, and adjustable structure create new opportunities in neurorehabilitation by enhancing the adaptability, precision of EEG-based monitoring and therapeutic interventions.

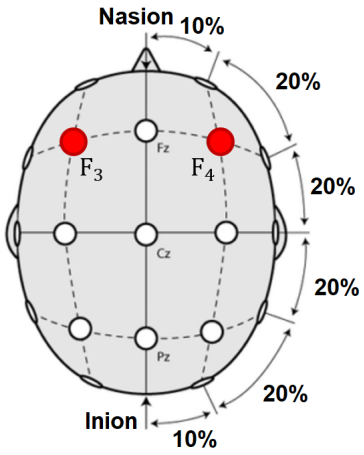


Figure 1. International 10–20 system.

The design of the Chameleon-1 helmet is presented with the following views and describes each part:

- Front part

This region includes most of the elements that make up the mechanical part of the Chameleon-1 helmet (see Figure 2), which is a vitally important area for the design, highlighting its main function in the capture of electrical signals generated by neurons; among other functions, the innovative mechanism with great versatility for different skull sizes stands out.

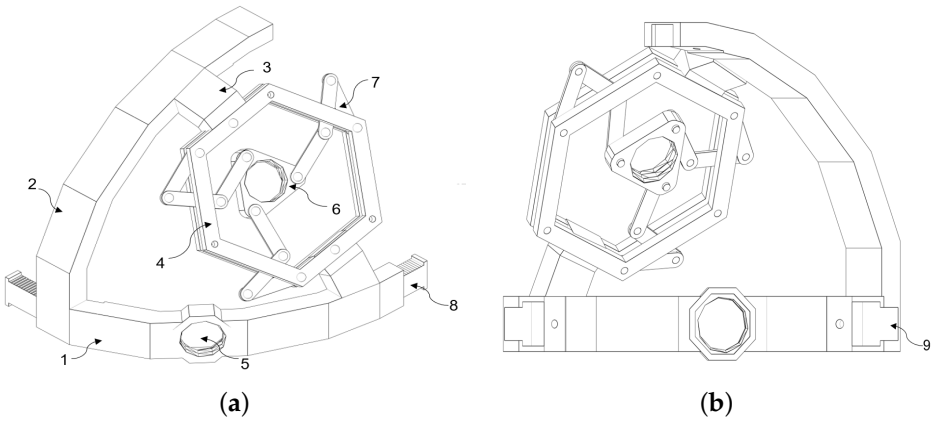


Figure 2. (**a**) External isometric view (front part), (**b**) internal isometric view (front part).

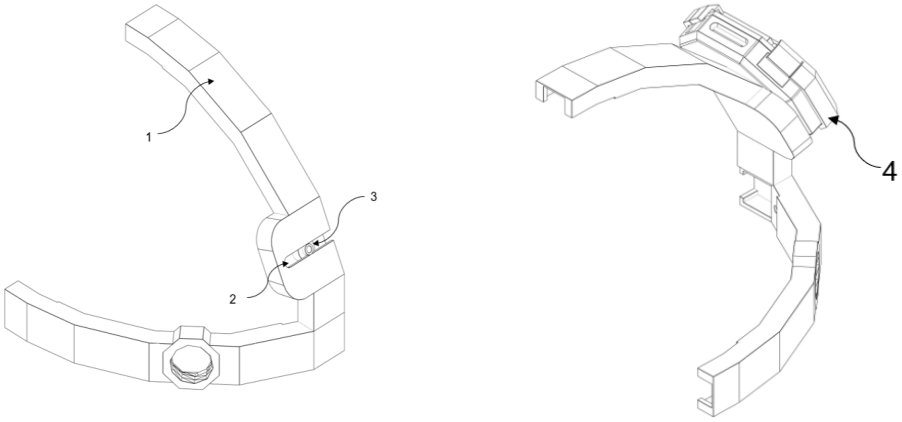
The front part of the helmet is made up of the following various pieces:

1. Base: This part of the helmet is responsible for adhering to the skull (which surrounds it and is adjustable for all types of skull). Its function is crucial, since it constitutes the base of the helmet, taking into consideration the minimum average size of a skull 50 cm in perimeter, considering the skull as an ellipse.
2. Column: This is the vertical part that holds most of the helmet's weight, which is attached to the aforementioned base. This adjusts to any type of skull. It offers the necessary support and flexibility to provide enough firmness for prolonged use.
3. Supports: This is one of the most important parts of the mechanism, as it connects the plane of movement of the column to the base. Its function is to keep the plane of movement in its position.

4. Movement plane: It is the hexagonal piece that generates a free virtual space where the electrode will have to move freely; the space has an area large enough to correctly adjust the electrode.
5. Weight distributor: It is a fixed slot created at the base of the helmet, which is designed to place a piece that has a direct connection between the skull and the base of the helmet, helping to distribute the weight of the helmet.
6. Sensor base: This is the most important part of the helmet. Its function is to hold the electrode and keep it fixed with the help of the arms for correct placement. The part includes three holes for connections with other parts as well as having a triangular shape to optimize its dimensions and make optimal use of the virtual space that delimits it.
7. Arm: It is the piece designed to connect the sensor base with the plane of movement. One of its functions is the mobility that it provides to the sensor base to adjust the electrode to the measurement point and to offer firmness to keep it in a correct measurement position.
8. Expansion mechanism: This is a designed piece that is placed inside the helmet's base to hold the base together. This piece is not fixed inside the base. This piece grants the ability to expand and can expand from a small helmet to a large one. The piece has a lateral relief that allows the mechanism to remain in an assigned position.
9. Slots: This is the space generated in the base and column. It is responsible for protecting and maintaining the expansion mechanism in position.

- Back part

This region of the helmet contains all the elements that make up the electronic part of the Chameleon-1 helmet (see Figure 3). It is a very important area of the helmet, whose function is to process and store electrical signals from the brain and then transmit the information to the computer.



(**a**) (**b**)

Figure 3. (**a**) External isometric view (back part), (**b**) internal isometric view (back part).

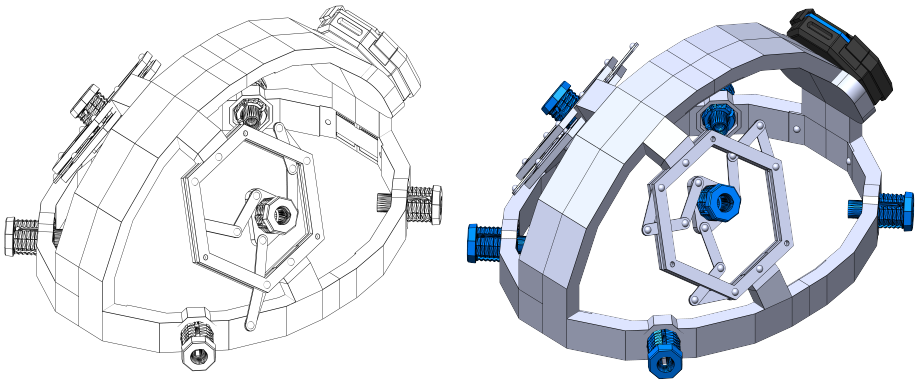
In addition to containing the other elements mentioned above, the back part has several modifications, which are described below:

1. Rear column: It is a modification of the front column; its main difference is an expansion close to the base, providing stability to the protective box of the plate.
2. Rear slot: This is a space created to protect the expansion cylinder, allowing mobility and firmness to the protection box. The expansion mechanism must be mobile so as not to affect the expansion.

3. Expansion cylinder: These are two pieces that are placed inside the rear slot; their function is to provide the necessary mobility and firmness to the protective box.
4. Protective box: This is the protective casing responsible for protecting the helmet's electronic board. Its function is to provide security and rigidity to the board in order not to compromise data collection.

Full 3D Chameleon-1 Helmet

The parts mentioned above make up the Chameleon-1 helmet (see Figure 4). The design features four bases, two front columns, four supports (two in each of the hemispheres), two motion planes, four weight distributors, two sensor bases, eighteen arms (nine in each hemisphere, grouped in three joints), four expansion mechanisms, twelve slots in the bases and columns, two rear columns, two expansion cylinders, and a protective case (see Figure 4a).



(**a**) (**b**)

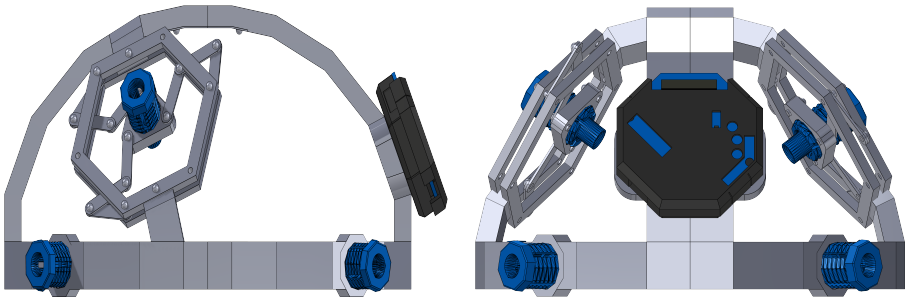
Figure 4. (**a**) Isometric view, (**b**) 3D isometric view of the Chameleon-1 helmet.

Currently, there are different EEG devices, each of which stands out for one or more features depending on the model. In the literature, different shortcomings of the devices made were observed, among which the most recurrent is the size and fixed positioning. Some designs have limited expansion, while the design of the Chameleon-1 helmet expands like no other, managing to go from a small-sized helmet to a large one, in addition to incorporating the mobility system, this being the most innovative point of the EEG helmet.

Current EEG helmet designs are limited to a specific size, have fixed electrodes, and are not very ergonomic. Some EEG helmets also have one or all three of the characteristics mentioned above. For this reason, an innovative design was developed that offers alternatives that can satisfy each of the needs that are lacking in the options that are developed or on the market with applications in the health sector.

The developed EEG cap is designed to accommodate multiple electrode positions within the extended 10–20 system, including F_3, F_4, AF_3, AF_4, F_1, F_2, F_5, F_6, FC_3, FC_4, FC_1, FC_2, F_C5, and FC_6. These regions are closely associated with cognitive processes, making them highly relevant for studies on brain activity. This configuration allows for flexible electrode placement, ensuring comprehensive coverage of the targeted cortical areas and facilitating accurate signal acquisition. Four support units were implemented to distribute the weight of the Chameleon-1 helmet. These characteristics can be observed in Figure 4b.

The four support units adhere to the skull and provide stability to improve the accuracy of the data obtained during treatment sessions in addition to efficiently distributing the weight, as seen below in Figure 5a. Different materials were used to build the helmet, such as polycarbonate, polyamide, polyester ether ketone (PEK), acrylonitrile–butadiene styrene (ABS), polyacetal, polyetherimide, fiberglass, carbon fiber, and galvanized aluminum.



(**a**) (**b**)

Figure 5. (**a**) The 3D view (front), (**b**) 3D back view of the Chameleon-1 helmet.

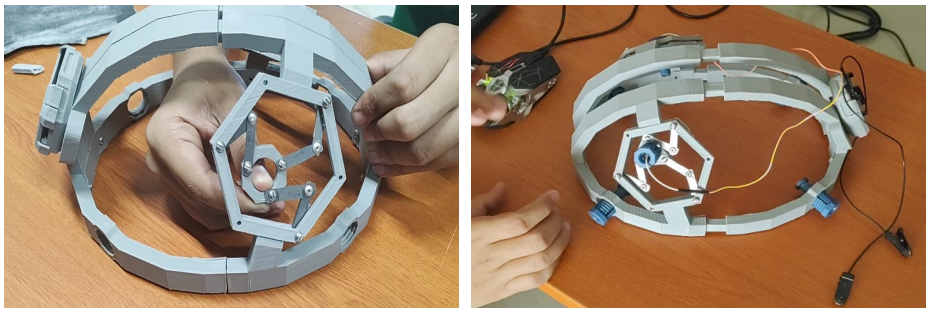
The back includes an eight-channel *OpenBCI* electronic board that uses a PIC32MX2 50F128B microcontroller, which samples at 250 Hz in each of the eight channels. The board is responsible for processing and storing the information obtained by the electrodes during therapy sessions. It also includes a protective casing whose main function is to protect the electronic board of the helmet, as shown in Figure 5b.

The helmet has a mechanism that allows expansion without difficulty, while the protective box remains fixed and attached to the helmet. These configurations and characteristics of the Chameleon-1 helmet help to have a good reading of the signals, generating reliability and stability to avoid significant data losses.

Building upon the developed design and addressing the limitations of existing headbands, efforts were focused on testing and characterizing the data obtained through the Chameleon-1 helmet. The following section provides a detailed analysis of this process.

3. Characteristics and Configuration of Chameleon-1 Headband

The Chameleon-1 helmet has certain characteristics that allow it to adapt and expand to different skull dimensions; on average, an 8-year-old child has a cranial perimeter of 35 cm (the Chameleon-1 helmet without expansion covers 34 cm of perimeter), while that of an adult on average is 56 to 58 cm (the Chameleon-1 helmet with its maximum expansion is 64 cm). Thus, it manages to cover almost all skulls, as shown in Figure 6a.



(**a**) (**b**)

Figure 6. (**a**) Chameleon helmet-1 without expansion, (**b**) expanded chameleon-1 helmet.

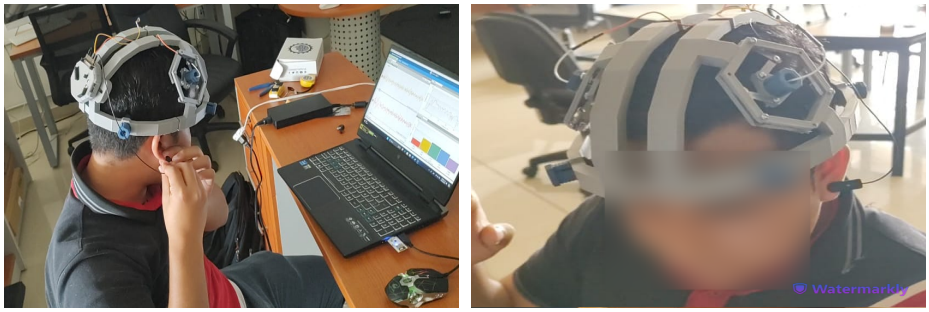
The electrodes of interest for this study are F_3 and F_4, as they are associated with cognitive processes, attention, and emotional regulation. These locations are particularly relevant for measuring brain activity related to concentration, relaxation, and stress detection.

For the correct placement of the Chameleon-1 helmet, a vertical measurement must be taken using a tape measure from the nasion to the inion. Then, the electrode positions F_3 and F_4 are identified following the 10–20 system, applying percentages relative to the obtained measurement. Specifically, to locate F_3, a point is marked on the left hemisphere

by taking 30% of the vertical distance from the nasion to the inion and 30% horizontally. The same procedure is applied for F_4 in the right hemisphere (see Figure 6b).

Figure 6 shows a complete view of the helmet and all the elements that make up its design, including two electrodes of the ear clip, which are placed in the earlobe to provide a reference and a ground signal. These elements reduce background noise and interference as well as improve the quality of the EEG signals obtained.

Once the two points to be measured have been identified, the base of the sensors is positioned at the correct points, as shown in Figure 7. The helmet is then placed and adjusted to the size of the skull of the patient who will wear it during therapy.



(**a**) (**b**)

Figure 7. (**a**) Placement of chameleon-1 helmet, (**b**) positioning of electrodes.

The points F_3 and F_4 were determined and are part of one of the four lobes of the brain, which is responsible for carrying out cognitive processes such as thinking, decision making, judgment, conflict resolution, attention, memory, and planning. These functions are related to the unique aspects to be studied and the analysis to determine their influence on neurological disorders.

Specialized OpenBCI software was used for the continuous monitoring and interpretation of data obtained in real time during therapy. The software features a wide variety of widgets, as shown in Figure 8, including the following:

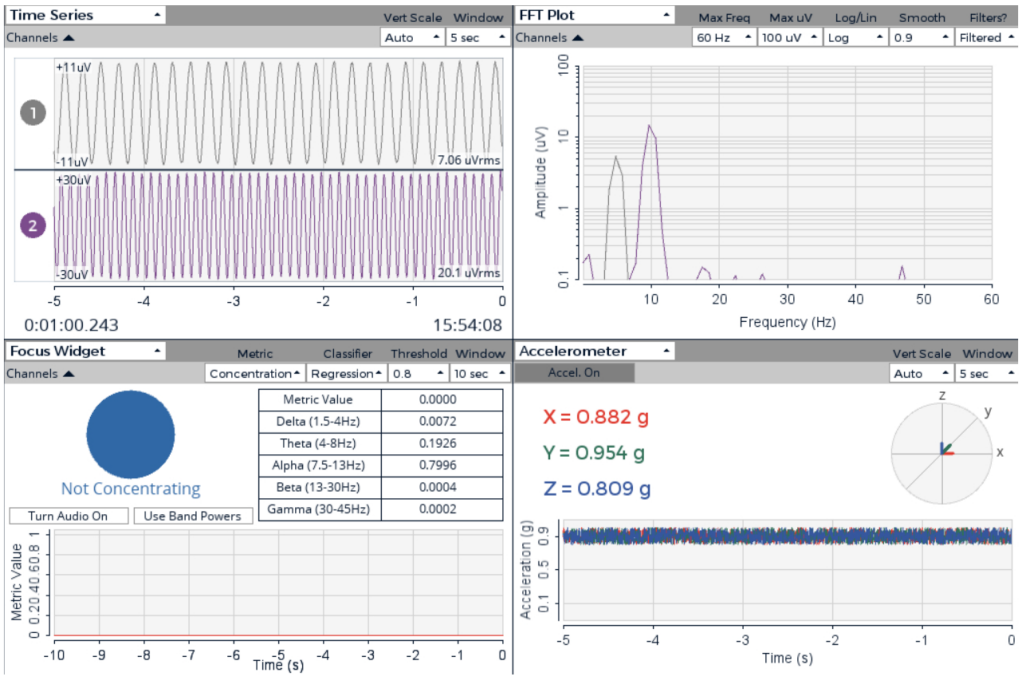


Figure 8. Graphic interface.

- Time series: This is the main widget for displaying biosensing data. It processes and displays the electrophysiological signal in real time, each graph representing the voltage detected at a given time by an electrode.
- Accelerometer: Each OpenBCI board is equipped with a three-axis accelerometer, whose data are transmitted to this widget. This accelerometer measures the acceleration of the board itself on an XYZ axis.
- Focus Widget: This feature uses the BrainFlow Metric feature to detect relaxation or concentration, which is also known as focus.
- FFT plot: This is a standard data visualization feature of bio-sensing tools. The x-axis shows various frequencies, and the y-axis shows the respective amplitudes of each frequency in microvolts. These amplitudes are displayed logarithmically by default.

The electronic part of the Chameleon-1 headset uses the openBCI cyton card to process and store EEG signals. From the data obtained, it is possible to classify the data according to the frequency and condition of the patients using the Chameleon-1 headset. The card has several characteristics that are mentioned in the following Table 1.

Table 1. Features of the openBCI cyton card.

Characteristics	Specs
Power	3–6 V
Microcontroller	PIC32MX250F128B
Analog Front End	ADS1299
Accelerometer	Lis3DH
Voltage Regulation	(3.3 V, +2.5 V, −2.5 V)
Board Dimensions	$2.41'' \times 2.41''$
Input Voltage Range	+2.5 to −2.5 V
Signal–Noise Ratio	121 dB

It is important to mention that the durability will depend on the use of the users and the conditions where the tests are carried out using the Chameleon-1 helmet. The helmet must be well managed and used so that it works without problems. In order for the materials to not suffer damage, it is advisable to place the helmet in protected areas and perform preventive maintenance when required. The materials with which the helmet was created have a durability of 10 years; however, if it becomes wet by accident, it can only last 1 year. The helmet has a wide gap due to its support points, as can be seen in Figure 2. At these points, piston-shaped pieces with a concave head (made of PLA-CF) and covered with cotton fiber are placed. The model or cover of the dry electrodes was manufactured with filament for 3D printing (PLA-CF). The part that makes contact with the skull is a cylindrical piece with small teeth made of stainless steel. Through this structure, it is possible to easily penetrate the hair to touch the patient's skull and take readings accurately. Different filters are considered to reduce the noise generated by the signals or conditions where the Chameleon-1 operates. These filters are as follows: Butterworth, Chebyshev, and Bessel.

After carrying out the design, manufacture and data acquisition of the Chameleon-1 helmet, experimental tests are performed with different patients to obtain adequate functioning of the Chameleon-1 helmet, which will be developed in the following section.

4. Results and Discussion

Validation using the Cameleon-1 helmet was carried out through several experimental tests. Preliminary results have shown that implementing an ergonomically optimized

design increases the reliability of the acquired signals, especially in prolonged monitoring applications.

This study analyzes cognitive activity using F3 and F4 electrodes, which are widely used in neurophysiological research for their effectiveness in EEG signal acquisition and the assessment of executive functions, attention, and cognitive processing.

To validate the helmet's effectiveness, brain oscillations in the delta (0.5–4 Hz), theta (4–8 Hz), alpha (8–12 Hz), beta (12–30 Hz), and gamma (>30 Hz) bands were analyzed, as they serve as biomarkers for various cognitive and physiological states. Specifically, the study examined conditions such as the following:

- Insomnia: increased beta and gamma activity during wakefulness, indicating cortical hyperactivation and difficulties in relaxation regulation.
- Stress: higher beta and gamma activity, which is associated with increased cortical excitability.
- Fatigue: increased theta and reduced beta activity, indicating cognitive slowing.
- High cognitive workload: increased theta and beta activity in prefrontal regions, reflecting sustained cognitive effort.
- High-performance athletes: higher alpha activity, which is linked to attentional regulation and cognitive efficiency.
- Healthy individuals: balanced spectral distribution.

Additionally, tests were conducted in relaxation and active states, where variations in alpha activity served as a reliable indicator. The helmet's stable and precise electrode placement allowed for more reliable recordings, enhancing its applicability in neurophysiological and clinical studies.

Table 2 presents the different EEG frequency bands and their association with various states of consciousness and neurophysiological activity in the subject.

Table 2. EEG frequency bands and their relation to consciousness states.

Wave	Frequency	State
Gamma	30–40 Hz	Concentration (problem resolution)
Beta	14–30 Hz	Attentive vigil
Alpha	7.5–14 Hz	Mental relaxation (rest)
Theta	3.5–7.5 Hz	Meditation (light sleep)
Delta	0.2–3.5 Hz	Deep sleep

4.1. Tests with Five Male Subjects with Different Brain Activity Conditions

The tests were carried out with five young participants in the age range of 19 to 25 years. EEG signals were monitored in real time. Five-minute sessions were conducted for each participant. Each section was divided into two phases; the first phase consisted of tracking the participant for 3 min in a state of concentration, and the second phase consisted of a period of 2 min in a state of relaxation. The data of the participants are shown in Table 3.

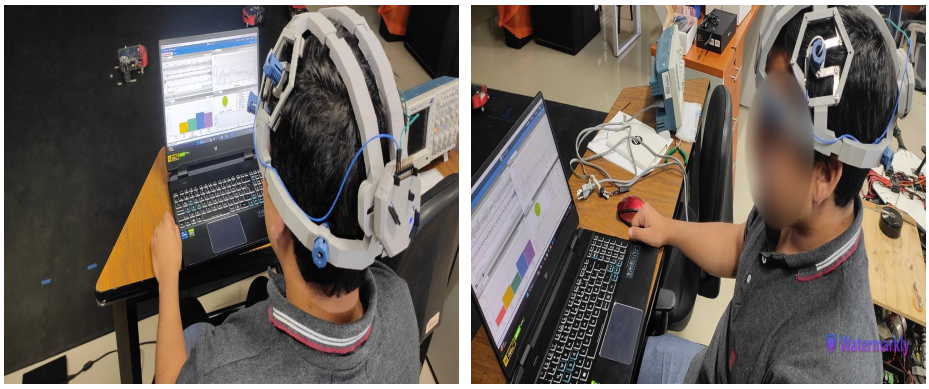
Table 3. Data from male participants using the Chameleon-1 helmet.

Patient	Gender	Health
Subject 1	Male	Healthy
Subject 2	Male	Healthy
Subject 3	Male	Moderate stress
Subject 4	Male	Moderate insomnia
Subject 5	Male	Healthy

The EEG signal processing in this study included a fourth-order Butterworth bandpass filter (0.5–60 Hz) to remove low-frequency drift and high-frequency noise along with an optional notch filter (50 Hz and 60 Hz) to eliminate power line interference. Furthermore, DC bias removal was achieved through common mode rejection (CMR) using the bias electrode as well as high-pass filtering (0.5 Hz cutoff) to eliminate slow drifts and offset, ensuring stable and high-quality EEG signal acquisition.

- Subject 1

First, the Chameleon-1 helmet is adjusted to the patient's skull, as seen in Figure 9a, and then the electrodes are adjusted at points F_3 and F_4 using the innovative movement mechanism of the Chameleon-1 helmet (see Figure 9b).



(**a**) (**b**)

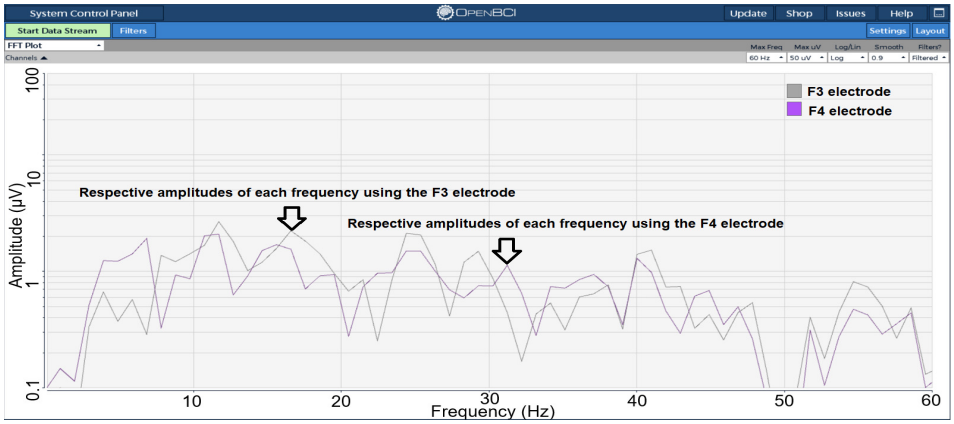
Figure 9. (**a**) Helmet placement, (**b**) start-up of tests with patient Subject 1.

In a time range (from 1 min to 2 min), normal voltage levels are observed at the points of interest; this is related to the previous information provided by the patient (without presenting levels of insomnia or stress), and this pattern can be observed in the OpenBCI program interface (see Figure 10). In the time series, a normal average voltage is observed in both channels (see Figure 10a), while Figure 10b shows the frequency spectrum. From the data acquired with the Chameleon-1 helmet, it is important to highlight that the patient exhibits an almost complete decrease in delta waves, approaching zero.



(**a**)

Figure 10. *Cont.*

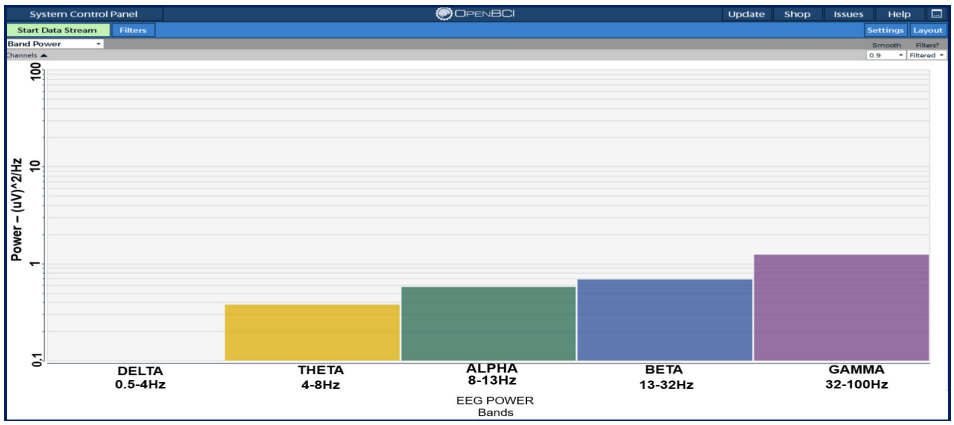


(**b**)

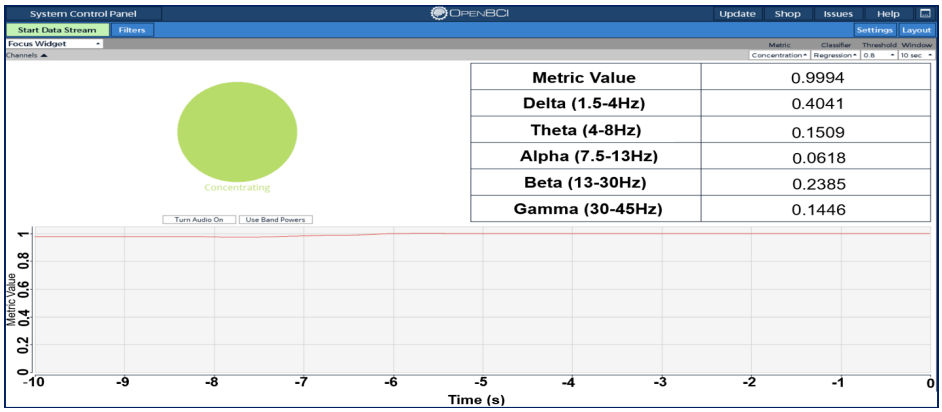
Figure 10. (**a**) Time series, (**b**) FFT plot of patient Subject 1.

A clearer understanding can be achieved by classifying each of the obtained signals by frequency (alpha, beta, gamma, delta, and theta). This allows us to observe the predominance of gamma and beta waves as well as delta waves that are nearly absent (see Figure 11a).

To monitor the two phases of the study (concentration and relaxation), the focus widget (default function) was used, and the results are shown in Figure 11b. The patient was observed to have no difficulty maintaining an optimal state of concentration (with minor variations).



(**a**)

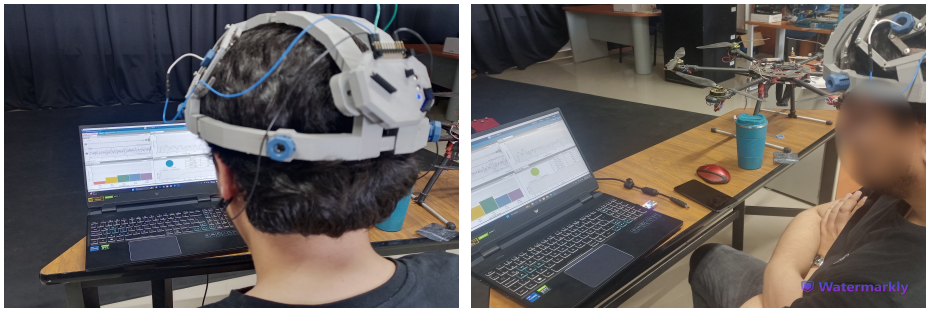


(**b**)

Figure 11. (**a**) Band power, (**b**) focus widget of Subject 1.

- Subject 2

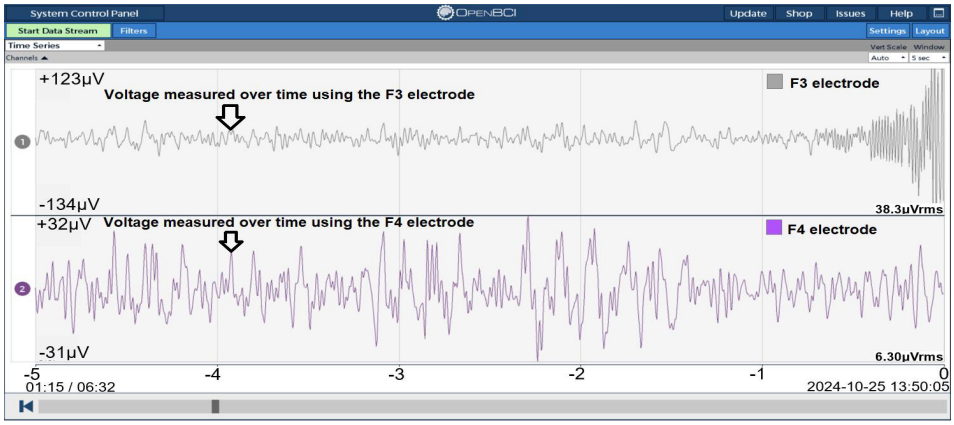
The test performed above is applied to the following patient, Subject 2. The 10–20 system was applied to place the Chameleon-1 helmet (see Figure 12a). A previous evaluation was performed and the patient was shown to be in good health (without stress or insomnia). In these characteristics, the results of the test with Subject 2 showed similarity to the results of Subject 1. Figure 12b shows Subject 2 wearing the Chameleon while performing the experiments.



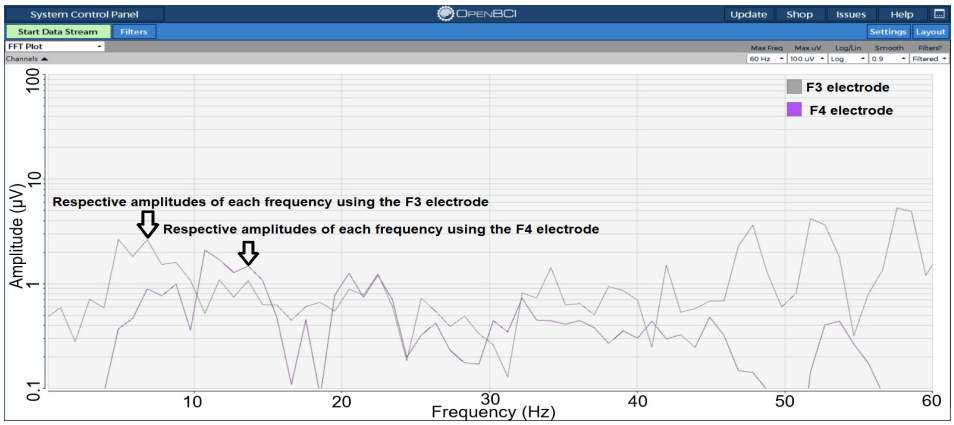
(**a**) (**b**)

Figure 12. (**a**) Helmet placement, (**b**) start-up of tests with Subject 2.

During the test, the patient was asked to blink rapidly to analyze how the signal changes with time, as can be seen in Figure 13a, and measure how blinking during the test can affect the incoming signal.



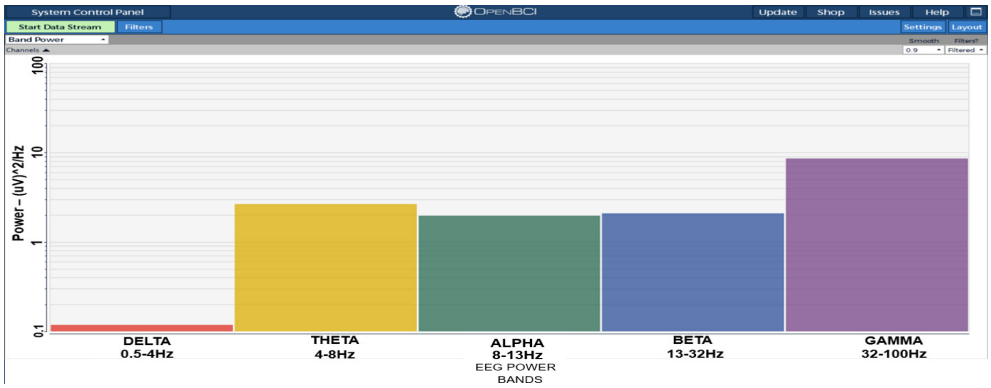
(**a**)



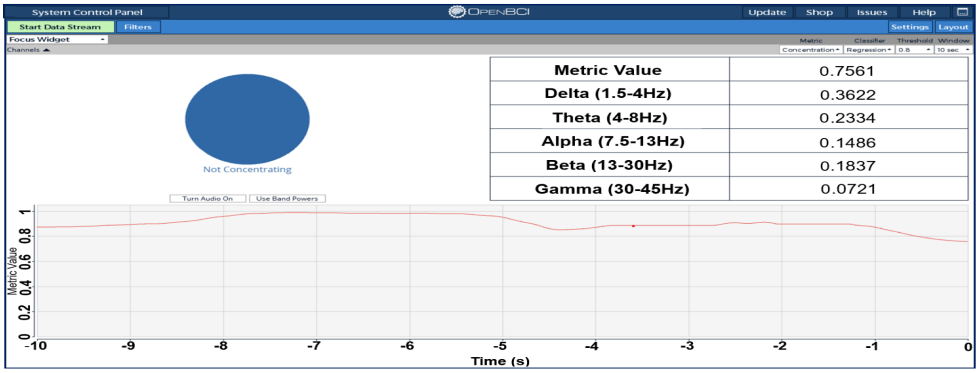
(**b**)

Figure 13. (**a**) Time series, (**b**) FFT plot of Subject 2.

In Figure 13b, an unusual increase in theta and gamma waves can be observed; this is due to the blinking requested from the patient during the session. In addition, an accumulation of gamma and beta waves can be observed, which is normal, since the patient did not show signs of ill health. Likewise, the real-time results of the classification of EEG waves during the session are obtained (see Figure 14a). At this stage, the patient was asked to solve mental mathematical problems, and it is possible to observe how gamma waves predominate during this variation of the test.



(**a**)



(**b**)

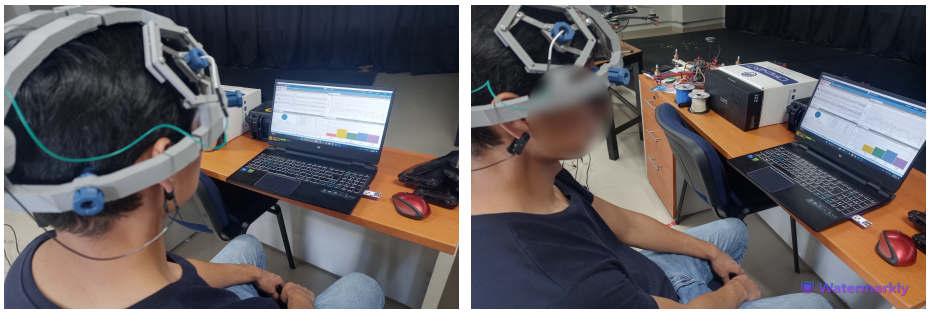
Figure 14. (**a**) Band power, (**b**) focus widget of Subject 2.

In Figure 14b, it can be observed that the patient has some difficulty maintaining a continuous state of concentration; however, the patient works to remain stable or close to a state without disturbance.

- Subject 3

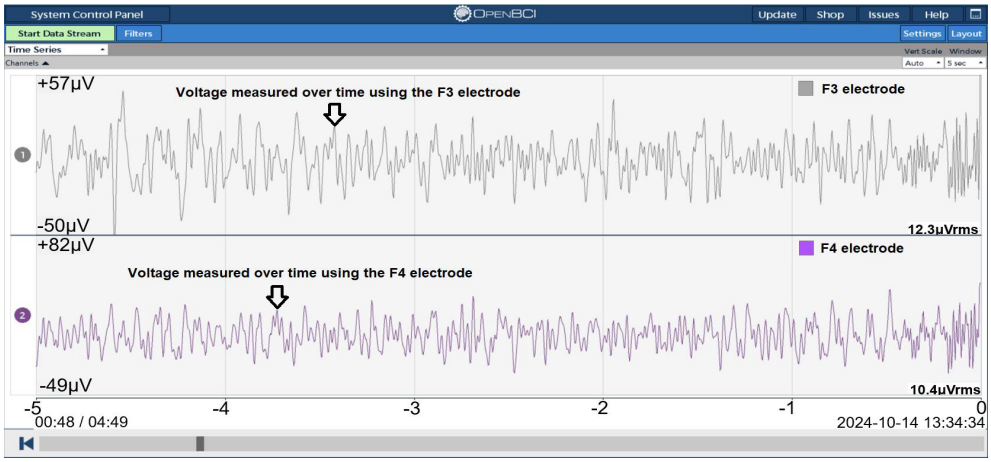
In Figure 15, we observe Subject 3. The results were different, since he presented a variation in his health status, which is moderately stressed due to his workload. The patient was not subjected to stress during the test. In this experimental test, priority was given to the relaxation phase based on breathing and meditation exercises through various instructions; the relaxation exercises were performed before the test.

The test started with a high level of electrical activity, as shown in Figure 16a; these data are consistent with the health status. The frequency spectrum was obtained, as shown in Figure 16b, revealing an accumulation of beta and alpha waves, along with a decrease in gamma waves, which occurs only at the beginning of the test. From these results, it was determined that the patient must be in an alert state since he will have difficulty concentrating and solving problems.

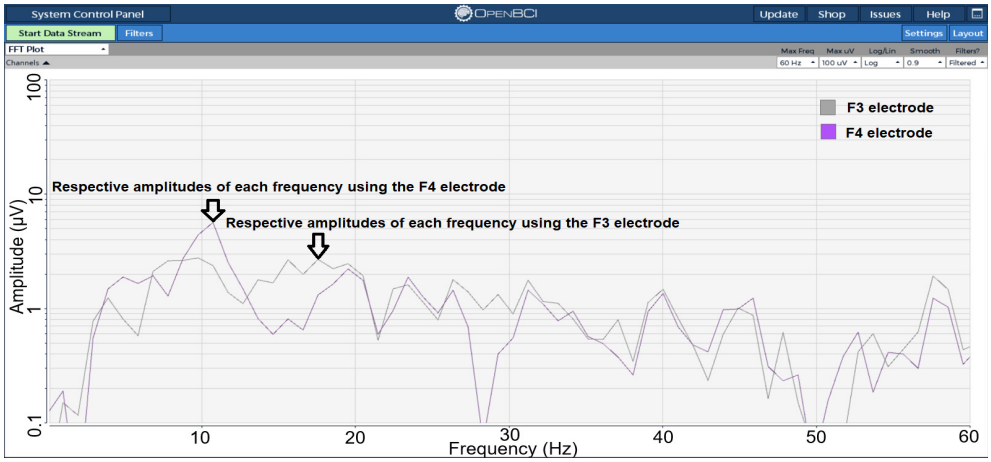


(**a**) (**b**)

Figure 15. (**a**) Helmet placement, (**b**) start-up of tests with Subject 3.



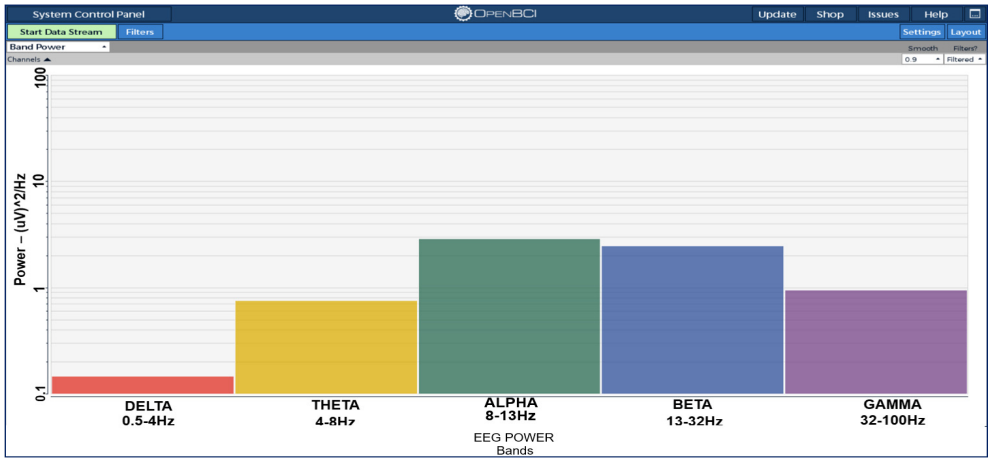
(**a**)



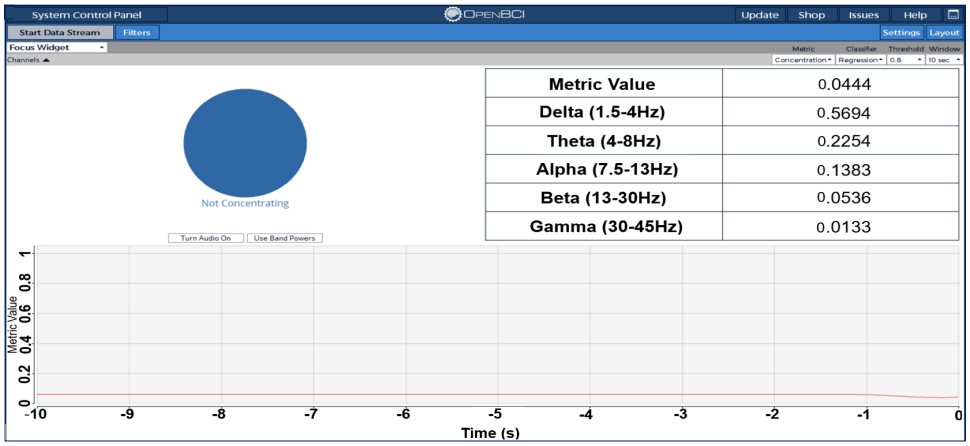
(**b**)

Figure 16. (**a**) Time series, (**b**) FFT plot of Subject 3.

Figure 17a shows the results obtained, as a total dominance of beta and alpha waves is observed, as well as a decrease in gamma waves; this is due to the moderate stress of the patient. Figure 17b shows another result; this is generated after the patient was subjected to the Chameleon-1 helmet test for 5 min, during which the patient was taken through a real-time monitored relaxation therapy, and an improvement in its signals is observed. From these results, it was possible to maintain a continuous state of relaxation during the last 3 min without difficulty.



(**a**)



(**b**)

Figure 17. (**a**) Band power, (**b**) focus widget of Subject 3.

- Subject 4

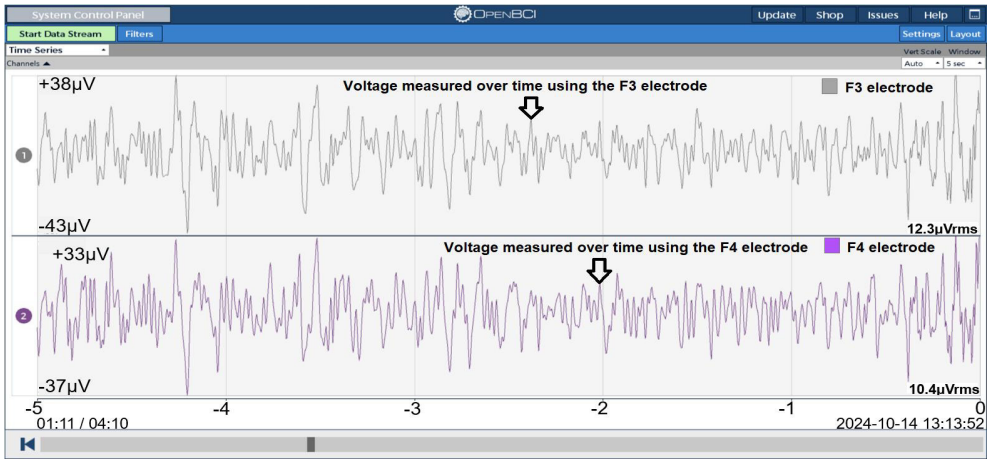
In this test, the patient exhibits a state of moderate insomnia due to a reduced sleep cycle (see Figure 18a). An interview was conducted to confirm his health prior to the test. In this test, the relaxation phase was prioritized based on breathing exercises and meditation based on several instructions, which were explained to the patient before the tests. There was no consumption of any type of drink or energizer that could modify his state of moderate insomnia.



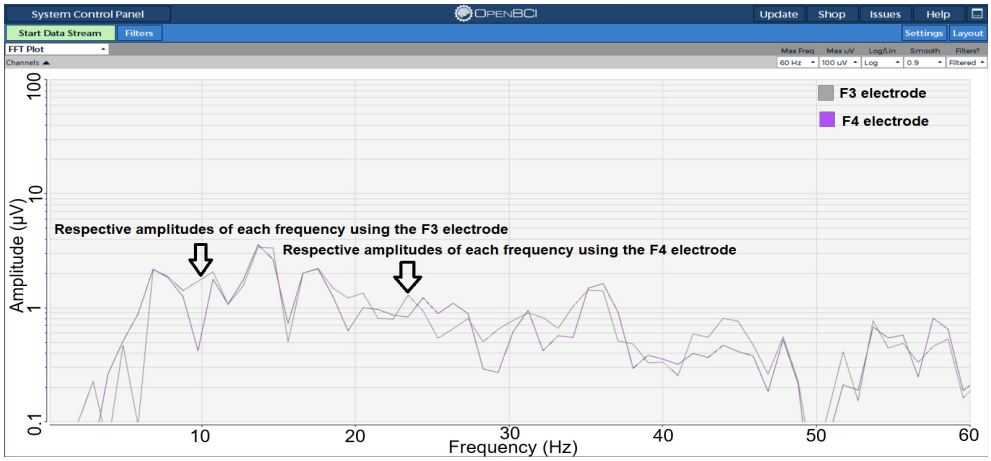
(**a**) (**b**)

Figure 18. (**a**) Helmet placement, (**b**) start-up of tests with Subject 4.

The test began with a low level of electrical activity, as shown in Figure 19a. These data suggest a possible relationship with the patient's health status, as the wave amplitude appears to be slightly below the range considered healthy in several observed periods. After 2 min, the test samples are taken and the results are shown in a graph of amplitude versus frequency, as seen in Figure 19b. Likewise, an absence of delta waves and a significant presence of theta waves can be observed, suggesting a state of fatigue in the patient. There is also an accumulation of beta and alpha waves as well as a decrease in gamma waves (only at the beginning of the test). With these data, it is possible to suggest that the patient may have difficulty concentrating and solving problems.



(**a**)

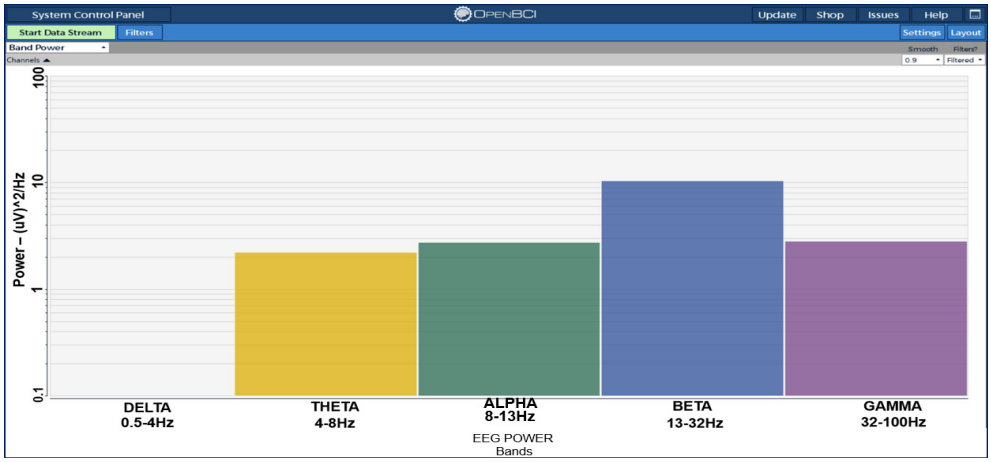


(**b**)

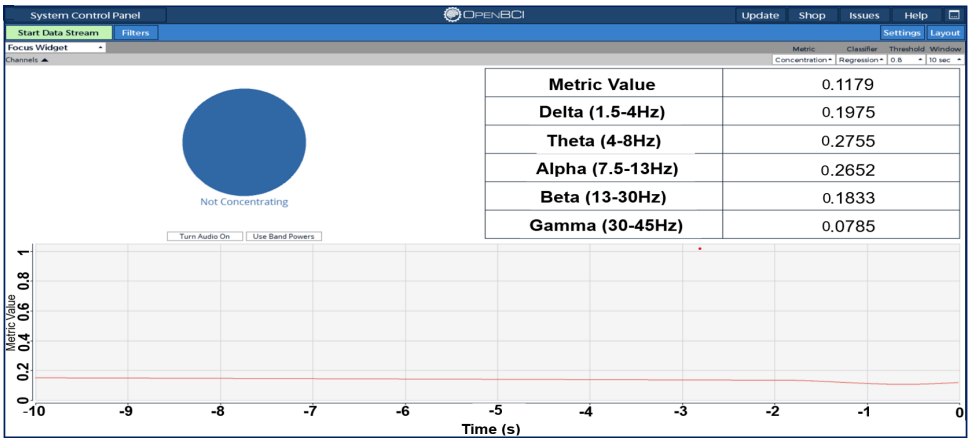
Figure 19. (**a**) Time series, (**b**) FFT plot of Subject 4.

Figure 20a corroborates our aforementioned results, showing a total dominance of beta waves, a decrease in gamma waves as a consequence of the patient's moderate insomnia, and a considerable increase in theta waves that are consistent with the patient's symptoms of light sleep.

Figure 20b shows other test results, in which after 5 min, the patient is guided through a relaxation therapy monitored in real time, and an improvement in results was achieved. Subject 4 maintained a continuous state of relaxation during the last minutes of the test.



(**a**)

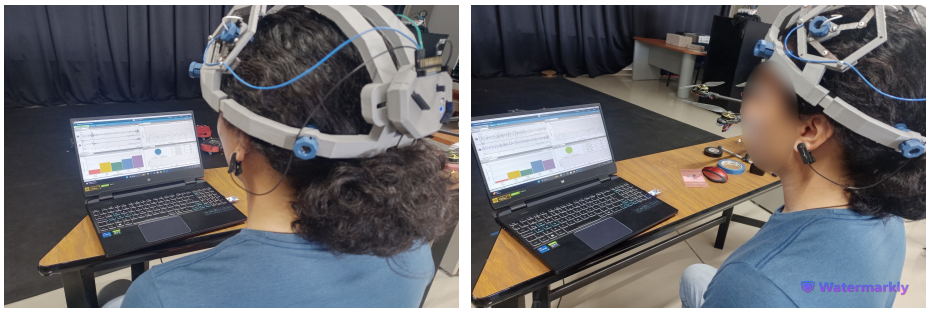


(**b**)

Figure 20. (**a**) Power band, (**b**) focus widget of Subject 4.

- Subject 5

The test began with an initial assessment of Subject 5 (see Figure 21a), suggesting a normal health status. Subsequently, a 3 min concentration session and a 2 min relaxation session were conducted as part of the experimental trials (see Figure 21b).

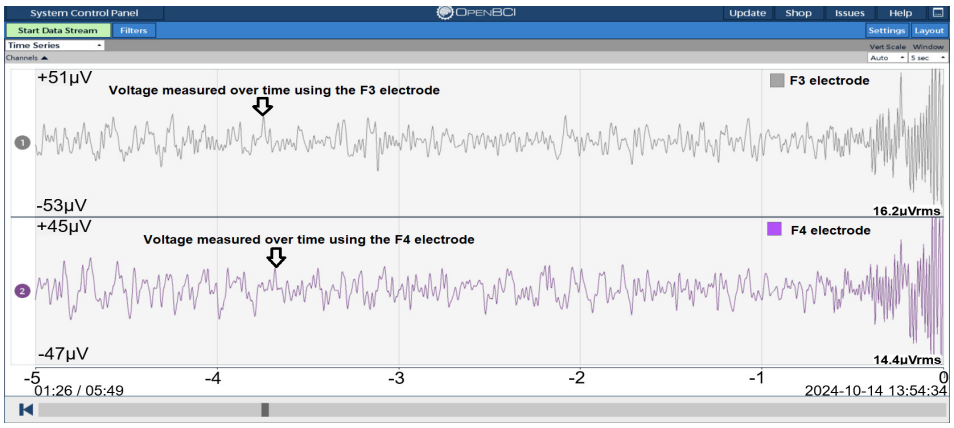


(**a**) (**b**)

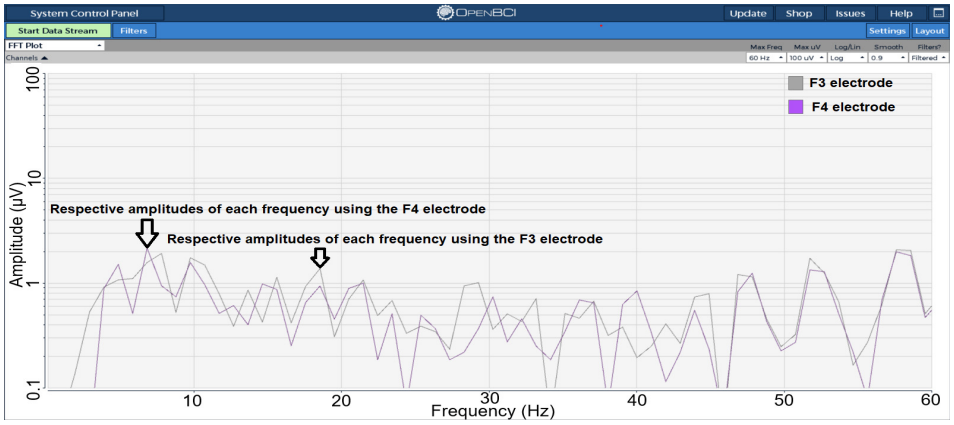
Figure 21. (**a**) Helmet placement, (**b**) start-up of tests with Subject 5.

Figure 22a presents the collection of patient data during a time of 1 to 2 min of the session. The amplitude of the sample is within the range that is considered a normal state of health. Both channels show similarity in the values obtained in real time. On the other

hand, in Figure 22b, the obtained data are observed, in which there is an accumulation of beta and gamma waves, in addition to a low accumulation of delta waves.



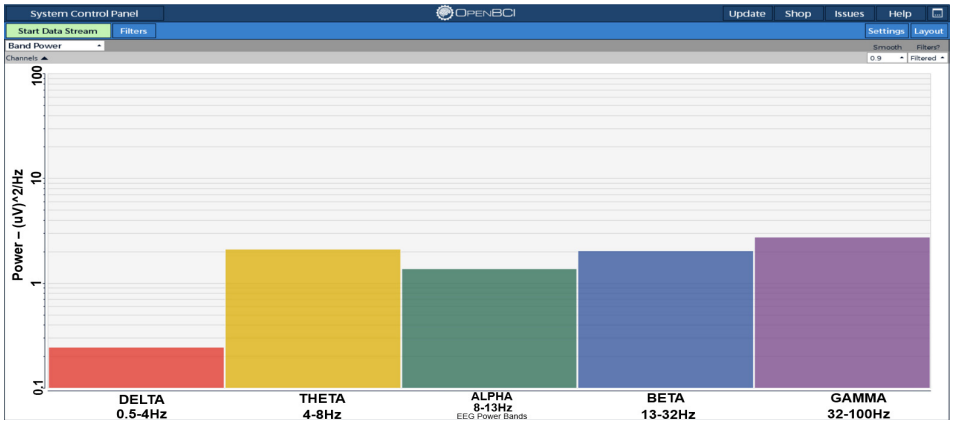
(**a**)



(**b**)

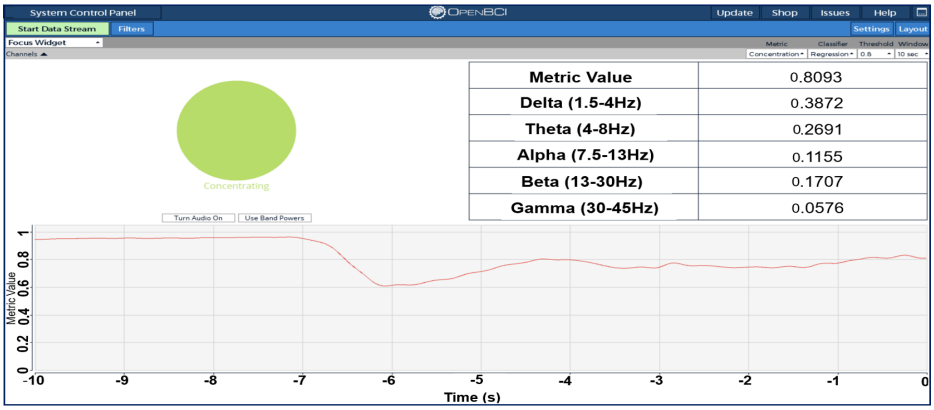
Figure 22. (**a**) Time series, (**b**) FFT plot of Subject 5.

The patient exhibited elevated gamma and theta bands along with a decrease in delta bands. As shown in Figure 23b, the patient had difficulty maintaining concentration, which may be associated with the increased theta activity and is often linked to fatigue or reduced cognitive focus.



(**a**)

Figure 23. *Cont.*



(**b**)

Figure 23. (**a**) Power band, (**b**) focus widget of Subject 5.

4.2. Tests with Four Female Subjects with Different Brain Activity Conditions

Four female subjects between 18 and 30 years of age were randomly selected to expand the sample and define the mobility performance of the electrode in the Chameleon-1 helmet. Participants were interviewed to obtain relevant information, such as age, health status before starting data collection, as shown in Table 4, and their medical history about any disease or injury related to the brain.

Table 4. Data from female participants who used the Chameleon-1 helmet.

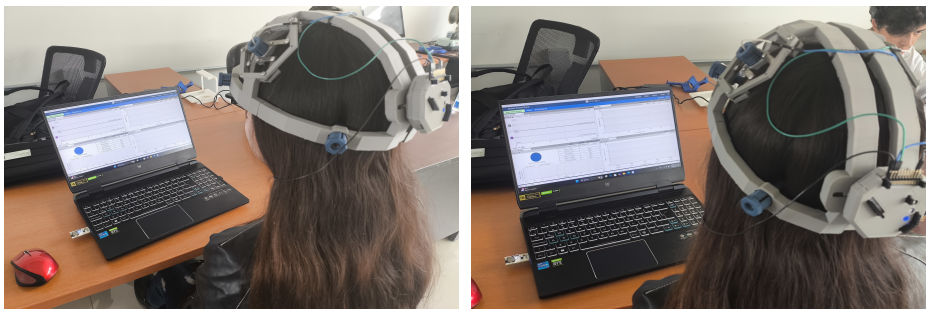
Patient	Gender	Health
Subject 6	Female	Moderate stress
Subject 7	Female	Moderate insomnia
Subject 8	Female	Healthy
Subject 9	Female	Healthy

Similar to the previous subjects, the EEG signals from female participants were processed using a bandpass filter (0.5–50 Hz), an optional notch filter (50 Hz and 60 Hz), and DC bias removal via common mode rejection (CMR) and high-pass filtering (0.5 Hz) to ensure signal stability.

- Subject 6

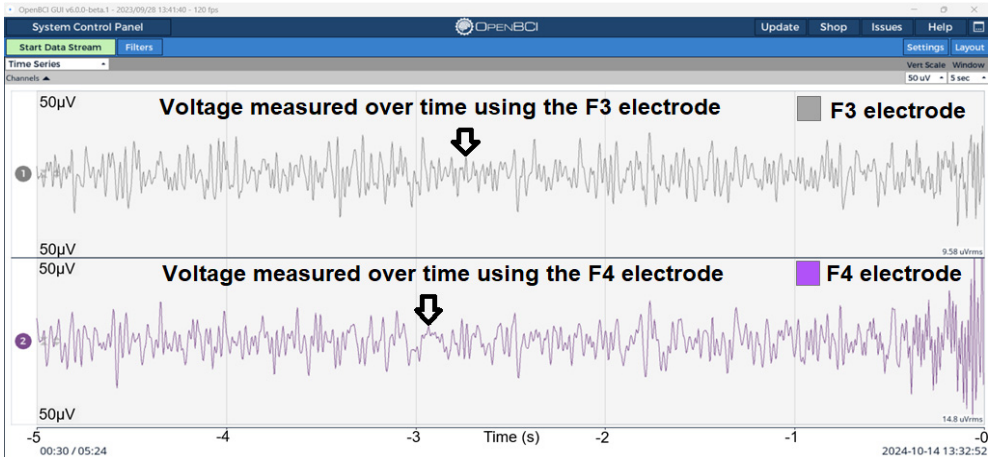
As in the male tests, the same methodology was carried out. The patient was first explained how the test would be performed (see Figure 24a). The patient was told that the test would last 5 min, which was divided into two stages of 3 min of concentration and 2 of relaxation. The patient was briefed on the software to be used (see Figure 24b), and a dedicated session was provided to address any questions.

Figure 25a shows the electrical activity of the brain. The voltage detected over time by electrodes F3 and F4 is presented. This is generated in a sample of 5 s. It should be noted that there were no data losses during the test, and the voltage recorded during the test is within a normal range. Figure 25b provides a sample of the data recorded from the patient, showing the amplitude as a function of frequency. The patient shows a greater amplitude in the alpha and theta bands than in the others.

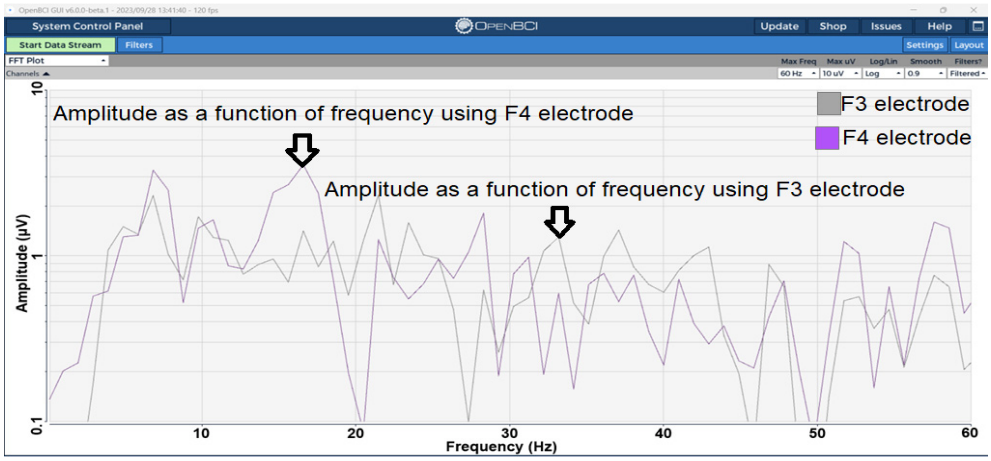


(**a**) (**b**)

Figure 24. (**a**) Helmet placement, (**b**) start-up of tests with Subject 6.



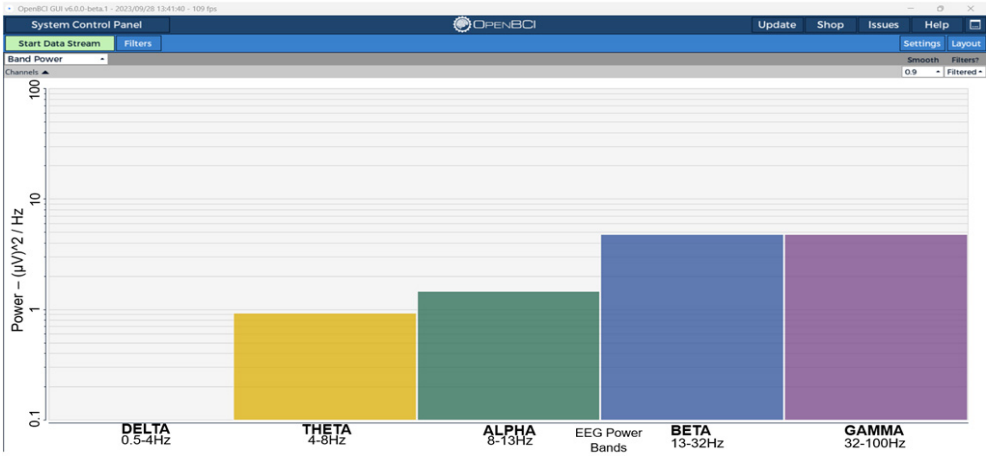
(**a**)



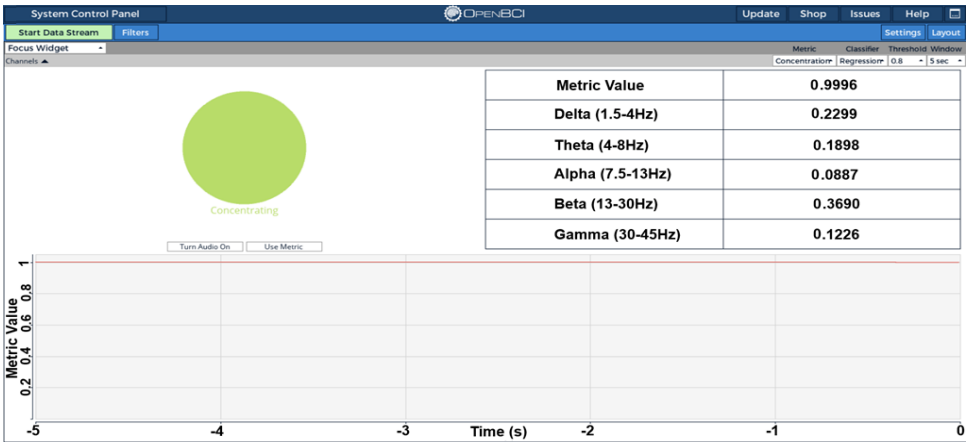
(**b**)

Figure 25. (**a**) Time series, (**b**) FFT plot of Subject 6.

Figure 26a shows an instant of the test performed, where beta and gamma waves predominate, indicating a moderate level of stress, and a null presence of the delta band. During the concentration test, the patient was asked to solve mental mathematical exercises and to perform breathing exercises during the relaxation round. Figure 26b shows the record obtained using the focus widget, highlighting the state of concentration with a red line shown on the metric value graph as a function of time.



(**a**)



(**b**)

Figure 26. (**a**) Power band, (**b**) focus widget of Subject 6.

- Subject 7

Figure 27a shows Subject 7, where the tests were conducted, and the data collection procedures were repeated. The same procedure was followed by collecting some relevant data from the patient, such as name, age, and a description of her health status at the time of starting the test. The helmet was then placed and adjusted, and its operation was explained (see Figure 27b).



(**a**) (**b**)

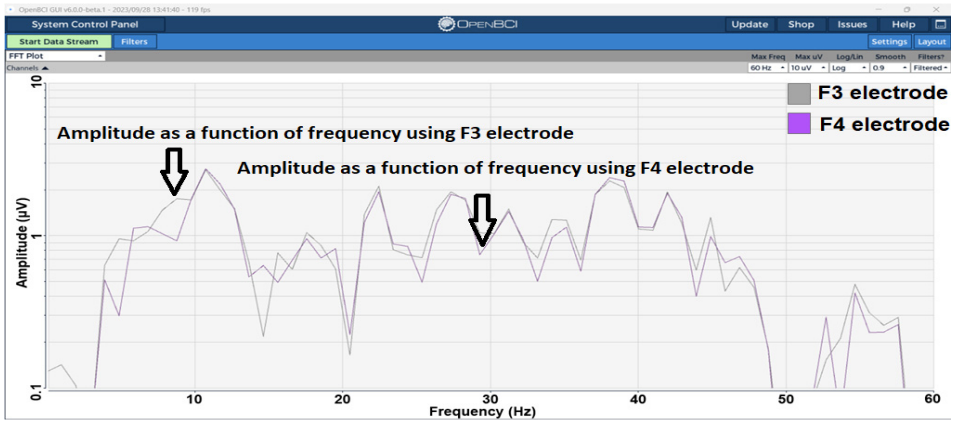
Figure 27. (**a**) Helmet placement, (**b**) start-up of tests with Subject 7.

During the first round of testing, the widget is set to 50 microvolts as the range to properly observe the signal obtained in both channels F3 and F4 (see Figure 28a).

In Figure 28b, the signal is distributed as a function of frequency. Theta is observed to have a greater presence.



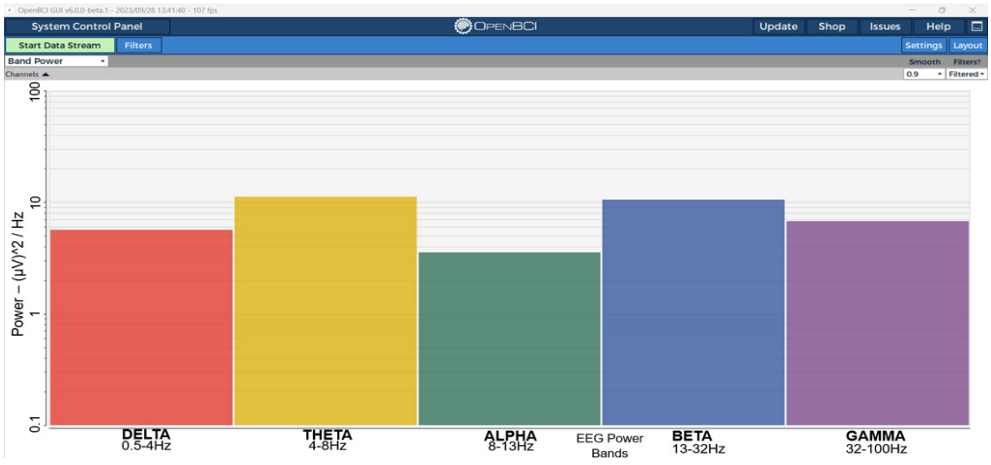
(**a**)



(**b**)

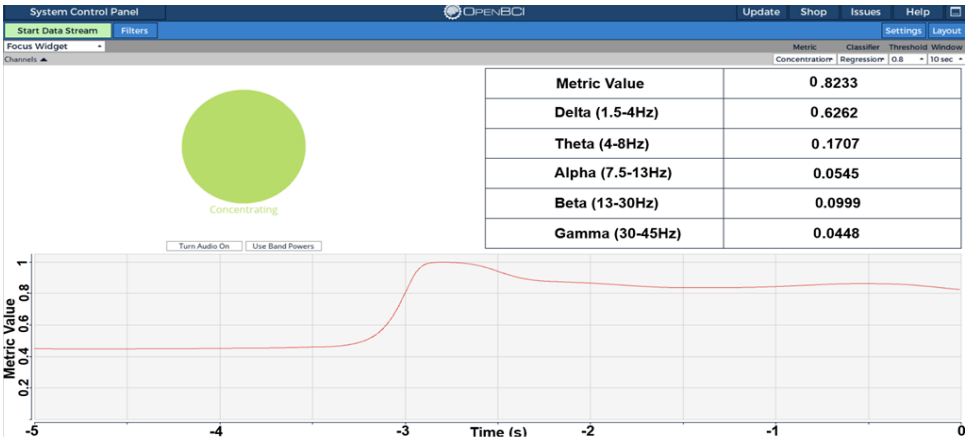
Figure 28. (**a**) Time series, (**b**) FFT plot of Subject 7.

In the concentration test, Figure 29a shows an increase in the delta and theta bands along with beta and gamma, suggesting a combination of insomnia and stress. Figure 29b shows that the patient has difficulty maintaining a constant state of concentration. During the relaxation round, the patient did not show any difficulty in performing the test.



(**a**)

Figure 29. *Cont.*



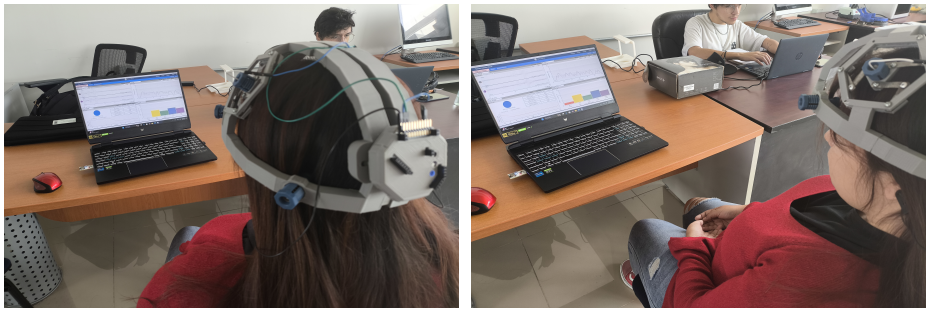
Metric Value	0.8233
Delta (1.5-4Hz)	0.6262
Theta (4-8Hz)	0.1707
Alpha (7.5-13Hz)	0.0545
Beta (13-30Hz)	0.0999
Gamma (30-45Hz)	0.0448

(**b**)

Figure 29. (**a**) Power band, (**b**) focus widget of Subject 7.

- Subject 8

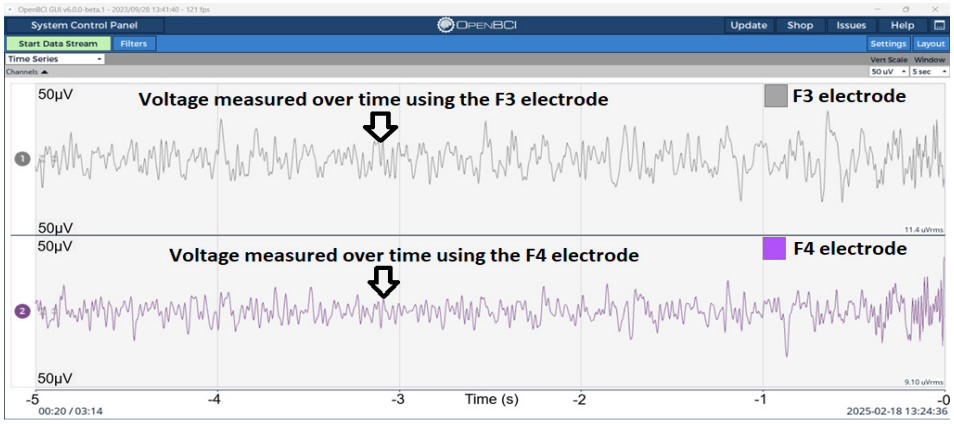
Figure 30 shows the penultimate patient (test Subject 8). Her data and records were taken as with the previous subjects. The helmet size was adjusted to the patient's skull. The electrodes were placed in the correct position for measurement. The interface was shown to the patient, and an explanation of the operation of the Chameleon-1 helmet was given.



(**a**) (**b**)

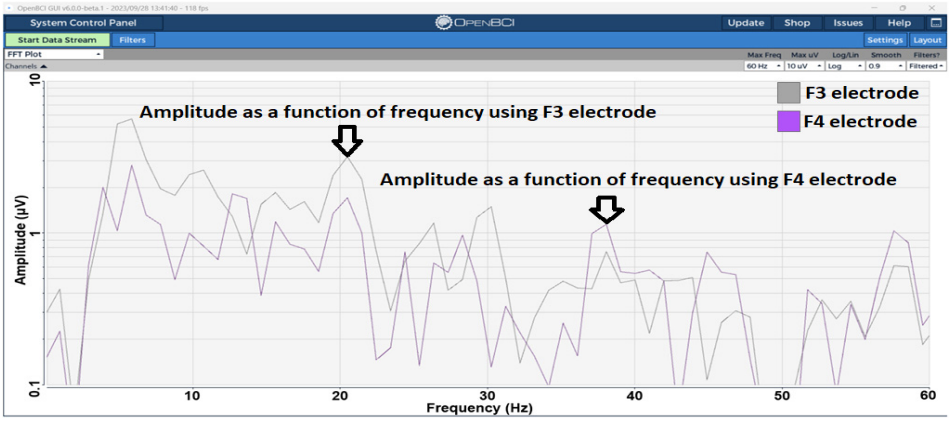
Figure 30. (**a**) Helmet placement, (**b**) start-up of tests with Subject 8.

During the analysis of the signal obtained, no anomalies are observed, as shown in Figure 31a. On the other hand, Figure 31b shows an increase in the amplitude of theta waves.



(**a**)

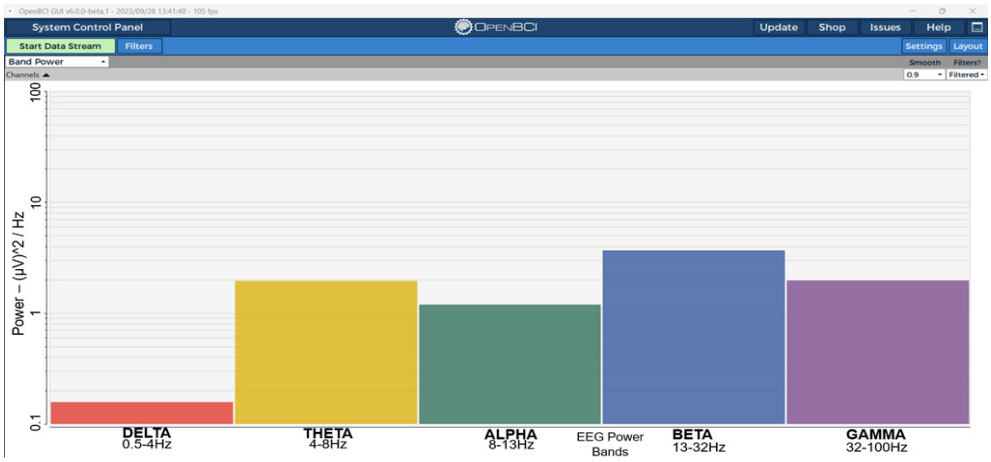
Figure 31. *Cont.*



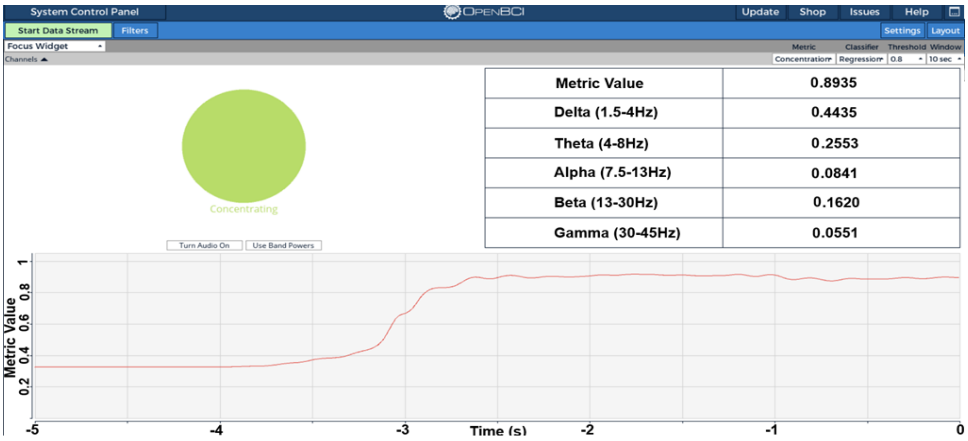
(**b**)

Figure 31. (**a**) Time series, (**b**) FFT plot of Subject 8.

During the first 2 min, the signal maintained constant behavior. As shown in Figure 32a, there was a small variation in the bands, but it maintained the tendency of beta and gamma as the main bands. In Figure 32b, the patient exhibited difficulty maintaining both concentration and relaxation states for extended periods.



(**a**)



(**b**)

Figure 32. (**a**) Power band, (**b**) focus widget of Subject 8.

- Subject 9

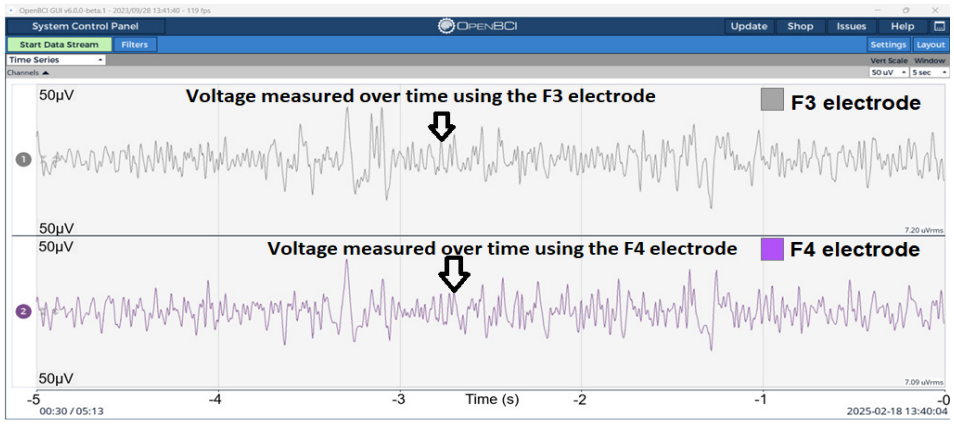
Figure 33a shows the last test Subject 8 using the Chameleon-1 helmet. A short interview was conducted to gather some data necessary for the analysis and interpretation of the signals that would be obtained. Then, with a tape measurer, the measurements were taken using the international 10–20 system to locate the points F3 and f4 (see Figure 33b). A short explanation of the helmet and the software was provided to the subject.



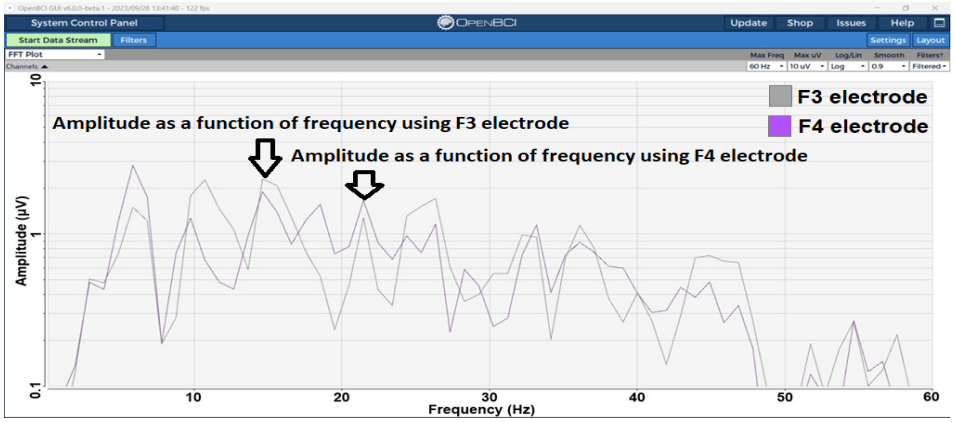
(**a**) (**b**)

Figure 33. (**a**) Helmet placement, (**b**) start-up of tests with Subject 9.

The program records the electrical activity of the brain whose amplitude range is limited to 50 microvolts in both channels. The signal obtained remains within the acceptable range, as shown in Figure 34a. The software uses filters to enhance the acquired signal, making it easier to visualize the amplitude across different frequency bands. In Figure 34b, a high theta signal and low beta and gamma activity are observed.



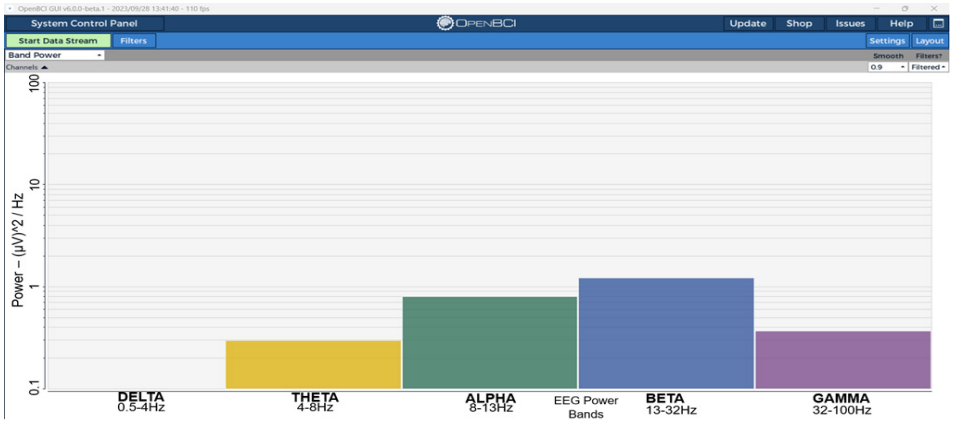
(**a**)



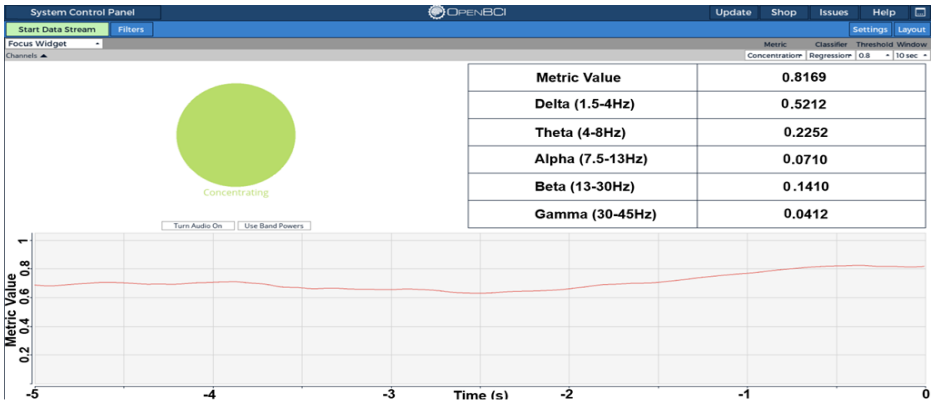
(**b**)

Figure 34. (**a**) Time series, (**b**) FFT plot of Subject 9.

Figure 35a presents a real-time representation of the frequency bands used to assess the concentration level of Subject 8. A predominant beta band is observed, which is generally associated with a state of alertness and active cognitive processing. This result is shown in Figure 35b, and a non-linear but constant concentration is observed. The relaxation stage was very similar to that of concentration. The purpose of these tests is to enhance concentration and, through a brief relaxation period, reduce stress to improve measurement accuracy and test efficiency.



(**a**)



(**b**)

Figure 35. (**a**) Power band, (**b**) focus widget of Subject 9.

However, the results are not sufficient to fully demonstrate the potential of the Chameleon-1 helmet. Therefore, to further support its efficiency and performance, positioning and power spectral density (PSD) tests were conducted in comparison with another commercial helmet. Specifically, the PSD of the alpha waves was analyzed to assess the relaxation state. This comparison is presented in the following subsection.

4.3. Comparison of Helmets

This study compares measurements between two commercial headsets, the Ultracortex Mark IV and Emotiv EPOC, and the one developed in this work, aiming to highlight the advantages of the proposed design over existing market models.

4.3.1. Positioning

Most commercial helmets have rigid structures and come in standard sizes such as small, medium, and large. Although these sizes are designed to approximate electrode

positioning according to international standards, they do not ensure precise alignment due to the variability in the shapes and sizes of the cranial joints.

This significant diversity in head shapes and sizes makes it difficult for a fixed-size design to fit properly across all anatomical configurations. Consequently, standard commercial helmets often do not position the electrodes accurately, which can affect the quality and precision of the measurements.

This study compares the actual positions of the F3 and F4 points, as defined by the international 10–20 system, with the electrode placements of the Ultracortex Mark IV and Emotiv EPOC headsets. The results indicate that these headsets do not always align precisely with the intended electrode positions, as shown in Figure 36 for the Ultracortex headset and Figure 37 for the Emotiv EPOC headset.

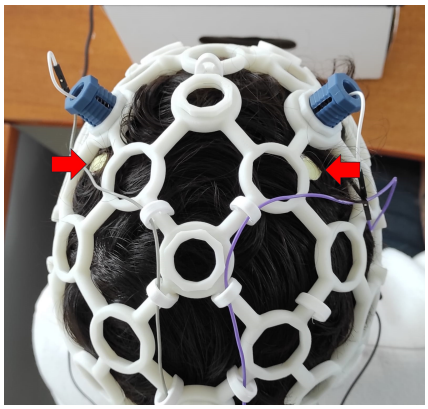


Figure 36. Comparison of the F3 and F4 electrode positioning according to the international 10–20 system and their placement in the Ultracortex helmet.



Figure 37. Comparison of the F3 and F4 electrode positioning according to the international 10–20 system and their placement in the Emotiv helmet.

Figures 36 and 37 illustrate how fixed-structure helmets can alter electrode positioning, while the Chameleon headset eliminates these discrepancies thanks to its adjustable electrodes, ensuring precise alignment. This is due to its ability to adapt to head width and allow electrode placement at different positions as needed, as shown in Figure 38.

The positioning error of the F3 and F4 points was evaluated based on 30 measurements for each headset, comparing the actual positions with those registered by the devices. For the Emotiv headset, the average error was 2.55 cm with a standard deviation of 0.97 cm. Meanwhile, the Ultracortex headset showed an average positioning error of 2.85 cm with a standard deviation of 0.784 cm.

It is crucial to note that the proposed helmet offers considerable versatility. Its electrodes can be easily placed at various locations within international reference sys-

tems, providing a significant advantage over other commercially available helmets with fixed configurations.

In addition, more tests with women are presented in Appendix A to demonstrate the versatility, effectiveness, efficacy, and great performance of the Chameleon-1 helmet.



Figure 38. Precise placement of the F3 and F4 electrodes using the Chameleon helmet.

4.3.2. Power Spectral Density in Alpha Waves

EEG signals, which researchers can measure using various methods, play a crucial role in multiple scientific and clinical applications. For example, researchers have effectively used the evoked potential of the P300 to control robotic devices [35]. In addition, EEG signals are widely used in diagnostic, prognostic, and therapeutic settings [36] and play a key role in human–machine interfaces for emerging technologies, such as soft exoskeletons for rehabilitation [37]. Furthermore, studies have shown that alpha waves correlate with relaxation states [38], and their detection offers promising potential for therapeutic interventions in the treatment of brain disorders [39]. Additionally, the Stockwell Transform, a time–frequency analysis technique, has proven effective in detecting evoked potentials like P300 as well as improving EEG signal processing and classification accuracy in brain–computer interface applications [40].

Various methods assess the functionality of a brain–computer interface system (BCI). In this case, validation occurs exclusively through alpha waves, which are known to increase when the subject reaches a state of relaxation.

Comparison Between Ultracortex and Chameleon

Three healthy subjects participated in the tests, each completing two trials: one using the Ultracortex Mark IV helmet and the other using the Chameleon-1 helmet. Each trial involved maintaining an active state (eyes open) for one minute, which was followed by one minute in a relaxed state (eyes closed). During the trials, the subjects remained seated, motionless, and followed the experiment's instructions. Figure 39 shows the three subjects and the helmets used in the experiments.

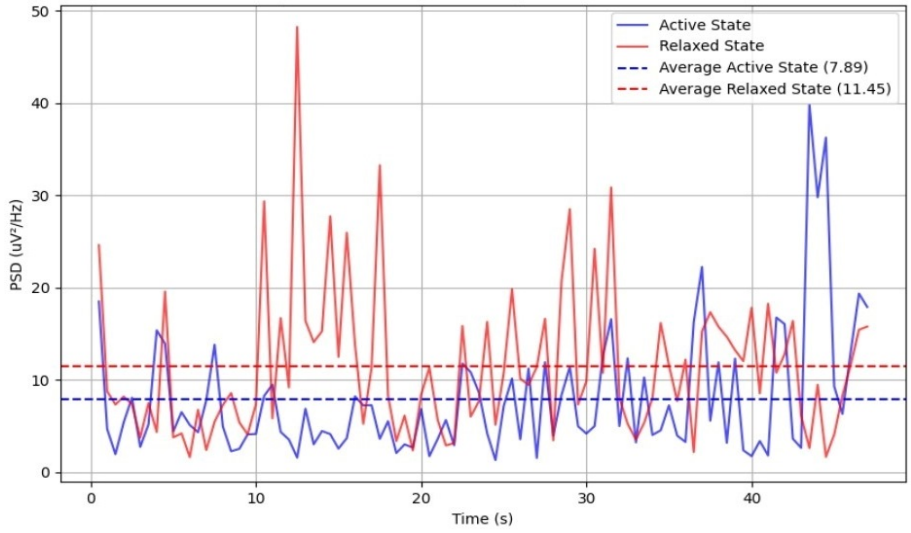
In the tests, data were collected from the F3 and F4 electrodes at a sampling rate of 250 Hz. Similarly to previous experiments, the EEG signals from the participants were processed using a bandpass filter (0.5–50 Hz), an optional notch filter (50 Hz and 60 Hz), and DC bias removal by common mode rejection (CMR) and high-pass filtering (0.5 Hz) to ensure signal stability. After filtering, the signals from both electrodes were combined to generate a single unified signal. A fourth-order Butterworth filter in the 8 to 13 Hz range was then applied to this signal. Then, a Fourier Transform (FFT) was performed to convert the signal into the frequency domain. Next, the signal's power spectral density (PSD) was calculated for each time interval within the 8 to 13 Hz range. Specifically, the values obtained within this frequency range were averaged at each time point so that each point

displayed the average spectral density for the 8 to 13 Hz frequencies. This process generated a representative value for the band in each interval during the two-minute test period.

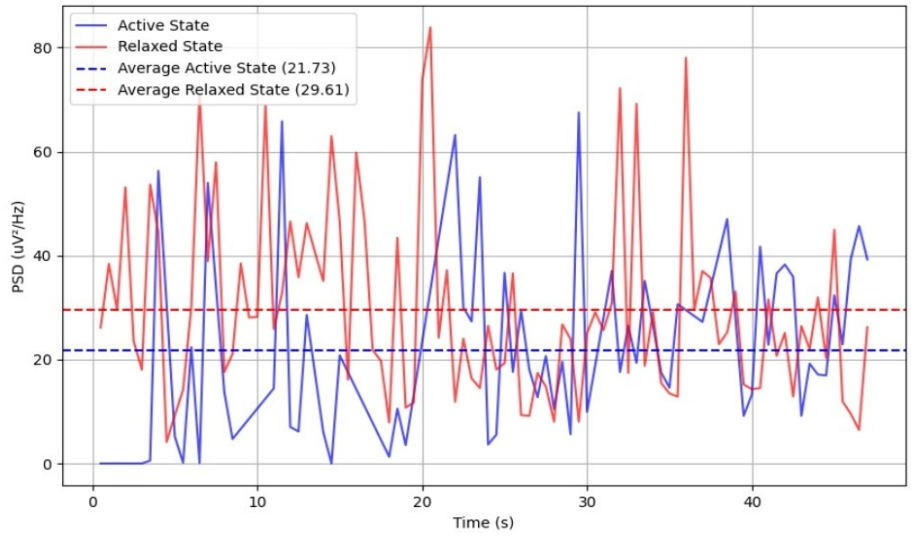


Figure 39. Healthy subjects used the commercial and Chameleon helmets in the experiments.

Each subject had two graphs, one with the commercial helmet and the other with the helmet developed in this paper. The graphs obtained for Subject 1 are shown in Figure 40.



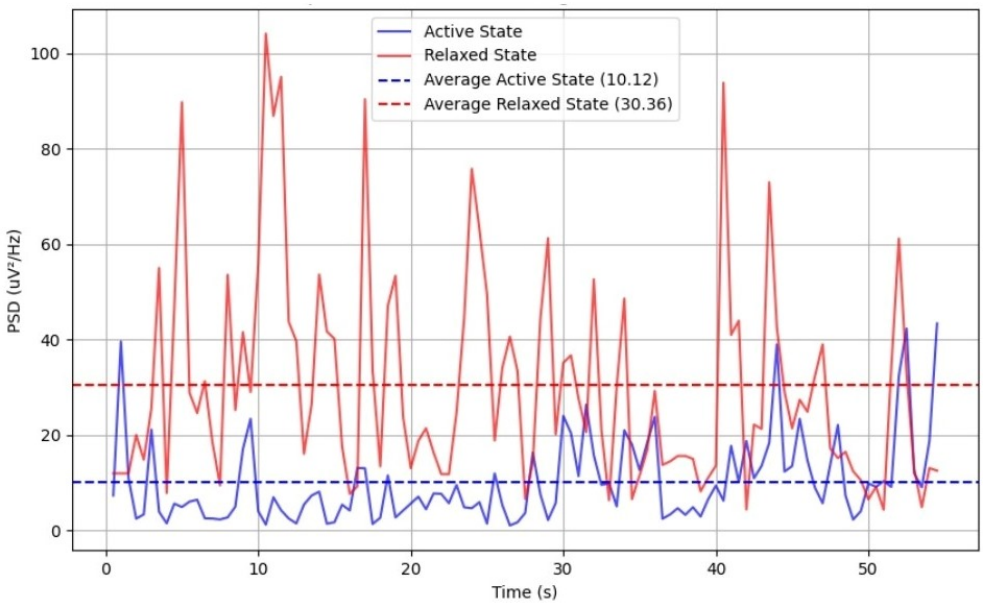
(**a**)



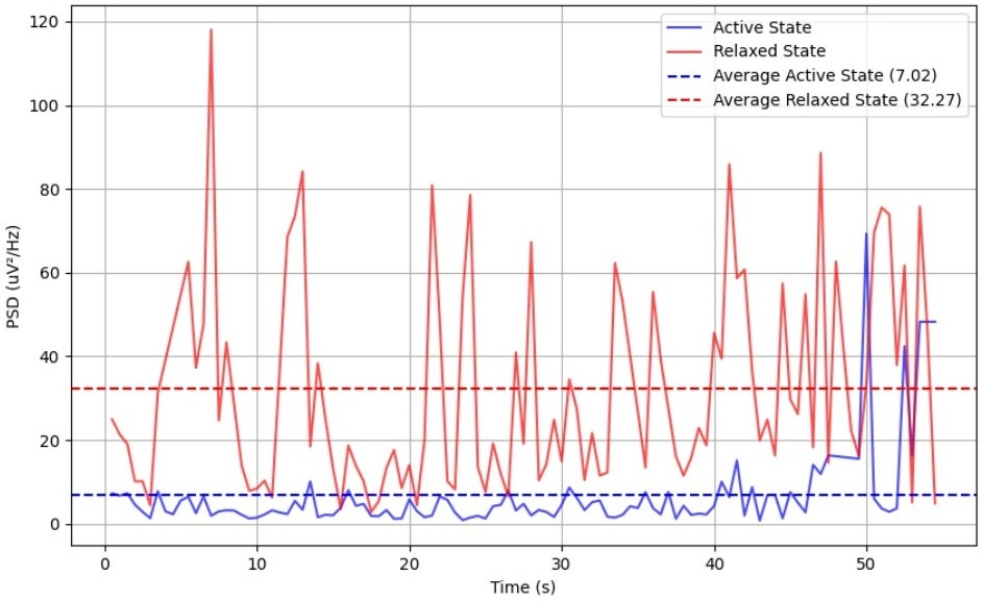
(**b**)

Figure 40. Alpha PSD (8 to 13 Hz) for Subject 1 (**a**) with the Ultracortex helmet, (**b**) with the Chameleon helmet.

Figure 40 shows the values obtained, where the active state produces lower PSD values than the relaxed state. For the Ultracortex headset, the average PSD reached 7.89 $\mu V^2/Hz$ in the active state and 11.45 $\mu V^2/Hz$ in the relaxed state, resulting in a difference of 3.56 $\mu V^2/Hz$. For the Chameleon headset, the average PSD measured 21.73 $\mu V^2/Hz$ in the active state and 29.61 $\mu V^2/Hz$ in the relaxed state, demonstrating a difference of 7.88 $\mu V^2/Hz$. These results confirm the expected behavior reported in the literature, showing an increase in PSD during the relaxed state. In particular, the Chameleon headset highlights a more pronounced difference between the two states, suggesting greater sensitivity to detect these variations. Figure 41 displays the graphs obtained for Subject 2.



(**a**)

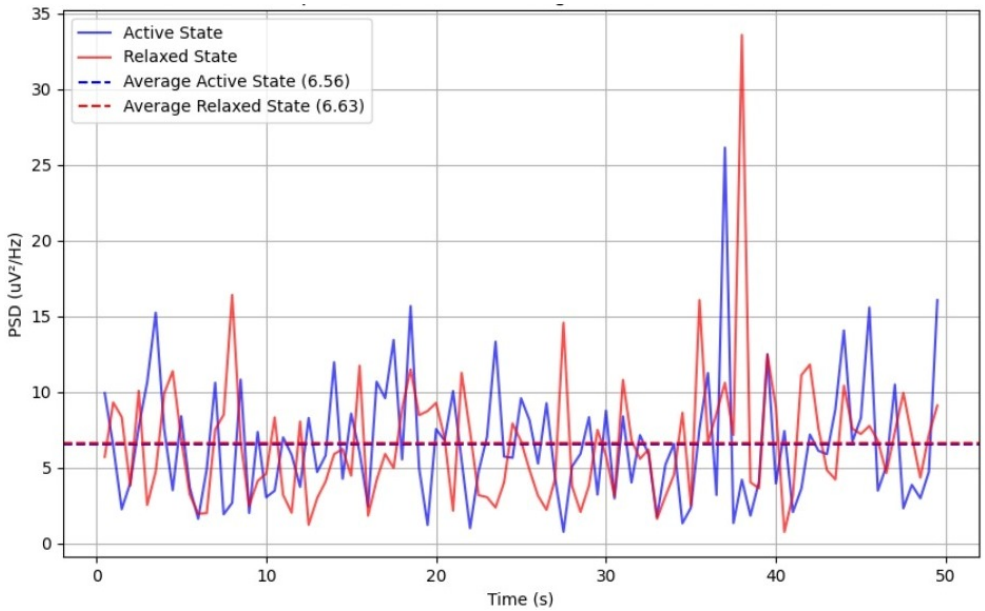


(**b**)

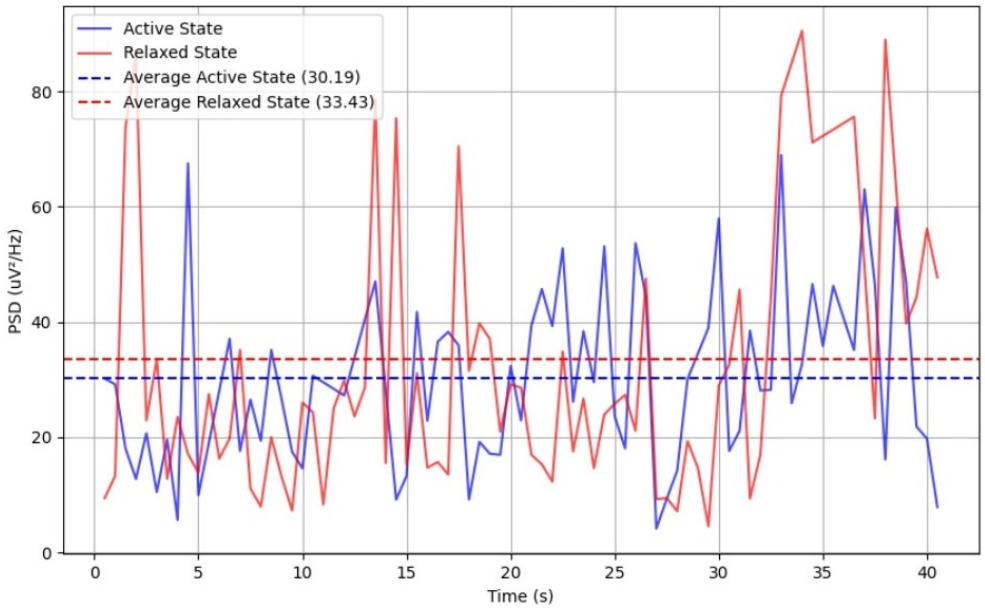
Figure 41. Alpha PSD (8 to 13 Hz) of subject 2 (**a**) with the Ultracortex headset, (**b**) with the Chameleon headset.

As shown in Figure 41, the values obtained for both headsets are within a similar range. For the Ultracortex headset, the average PSD was 10.12 $\mu V^2/Hz$ in the active state and

30.36 $\mu V^2/Hz$ in the relaxed state, with a difference of 20.24 $\mu V^2/Hz$. However, the Chameleon headset recorded an average of 7.02 $\mu V^2/Hz$ in the active state and 32.27 $\mu V^2/Hz$ in the relaxed state with a difference of 25.25 $\mu V^2/Hz$. These results again highlight a substantial difference between the active and relaxed states of the Chameleon headset, reinforcing its superior ability to discriminate between the two states. For Subject 3, the graphs shown in Figure 42 were obtained.



(**a**)



(**b**)

Figure 42. Alpha PSD (8 to 13 Hz) of subject 3: (**a**) with the Ultracortex headset, (**b**) with the Chameleon headset.

Graphs for Subject 3 indicate that the signals recorded during active and relaxed states were similar. This similarity significantly hindered the ability to distinguish between the two states, which could be due to several factors. One of the primary reasons may be the subject's difficulty in attaining a proper state of relaxation.

Regarding the Ultracortex headset, the average PSD was 6.56 $\mu V^2/Hz$ in the active state and 6.63 $\mu V^2/Hz$ in the relaxed state with a minimal difference of only 0.07 $\mu V^2/Hz$. This result suggests an almost nonexistent ability to differentiate between the two states.

In contrast, when using the proposed headset, the PSD was 30.19 $\mu V^2/Hz$ in the active state and 33.43 $\mu V^2/Hz$ in the relaxed state with a significant difference of 3.24 $\mu V^2/Hz$. Although this difference is slight, it is more meaningful in terms of the ability to discriminate between the two states than the commercially available headset. In Table 5, the mean PSD values and standard deviations (SDs) for the different subjects are presented for both helmets.

Table 5. Comparison of mean and standard deviation (SD) for power spectral density (PSD) in the 8–13 Hz range between Ultracortex and Chameleon helmets.

Helmet	Subject	Mean PSD (Active State) $\mu V^2/Hz$	SD PSD (Active State) $\mu V^2/Hz$	Mean PSD (Relax State) $\mu V^2/Hz$	SD PSD (Relax State) $\mu V^2/Hz$
Ultracortex	1	7.89	6.74	11.45	8.73
	2	10.12	8.96	30.36	22.17
	3	6.56	4.12	6.63	4.30
Total Mean		**8.19**	**6.61**	**16.15**	**11.73**
Chameleon	1	21.73	14.87	29.61	17.94
	2	7.02	10.85	32.27	23.80
	3	30.19	14.58	33.43	23.01
Total Mean		**19.65**	**13.43**	**31.77**	**21.58**

Table 5 presents the results obtained from the three subjects, showing their mean PSD values and standard deviations, as well as the total values for each helmet.

For example, the mean PSD for the Ultracortex helmet in the active state was 8.19 $\mu V^2/Hz$, while in the relaxed state, it reached 16.15 $\mu V^2/Hz$, resulting in a difference of 7.96 $\mu V^2/Hz$. In contrast, the Chameleon helmet had a total mean PSD of 19.65 $\mu V^2/Hz$ in the active state and 31.77 $\mu V^2/Hz$ in the relaxed state with a difference of 12.12 $\mu V^2/Hz$. This greater difference confirms the superior ability of the Chameleon helmet to distinguish between both states.

This study highlights the importance of alpha waves as an indicator of relaxation in BCI systems. The Chameleon-1 headset demonstrated a superior ability to discriminate between active and relaxed states with alpha waves, showing significant PSD differences in Subjects 1, 2, and 3, validating its effectiveness.

Comparison Between Emotive and Chameleon

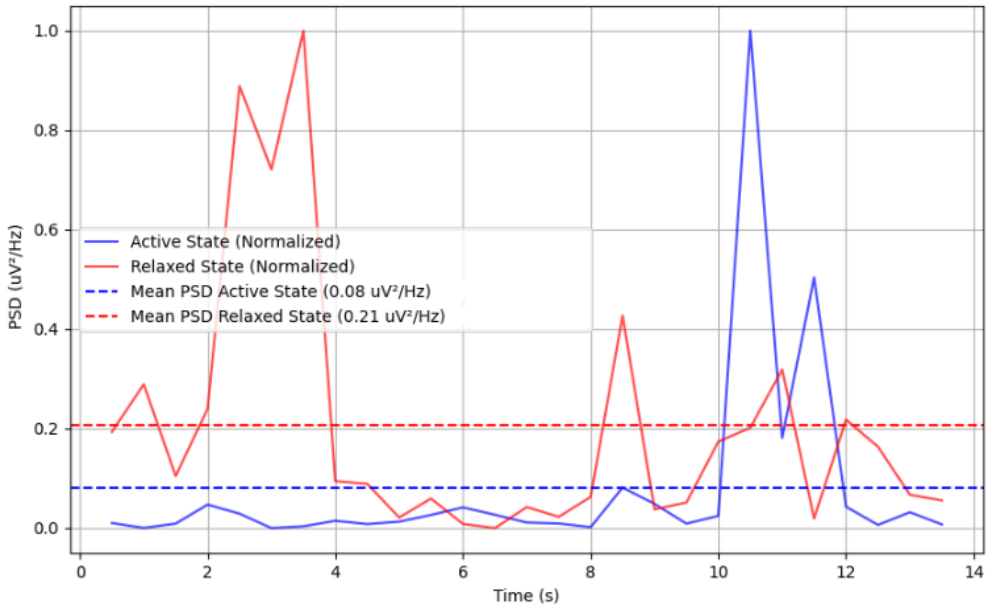
In this case, the process was similar to previous experiments but with a shorter recording time of 26 s: 13 s in an active state (eyes open) and 13 s in a relaxed state (eyes closed). Data were collected from the F3 and F4 electrodes at a sampling rate of 128 Hz. The EEG signals were preprocessed using bandpass filtering (0.5–50 Hz) and notch filters at 50 Hz and 60 Hz. Subsequently, the signals were combined into a single unified signal and processed with a fourth-order Butterworth filter (8–13 Hz). Then, a Fourier Transform (FFT) was performed to convert the signal into the frequency domain. Finally, the power spectral density (PSD) was calculated and normalized for analysis.

The tests were conducted on three young subjects, all women, aged between 19 and 21 years, as shown in Figure 43. These subjects were identified as 3, 4, and 5, maintaining continuity with the tests conducted in the previous subjects.

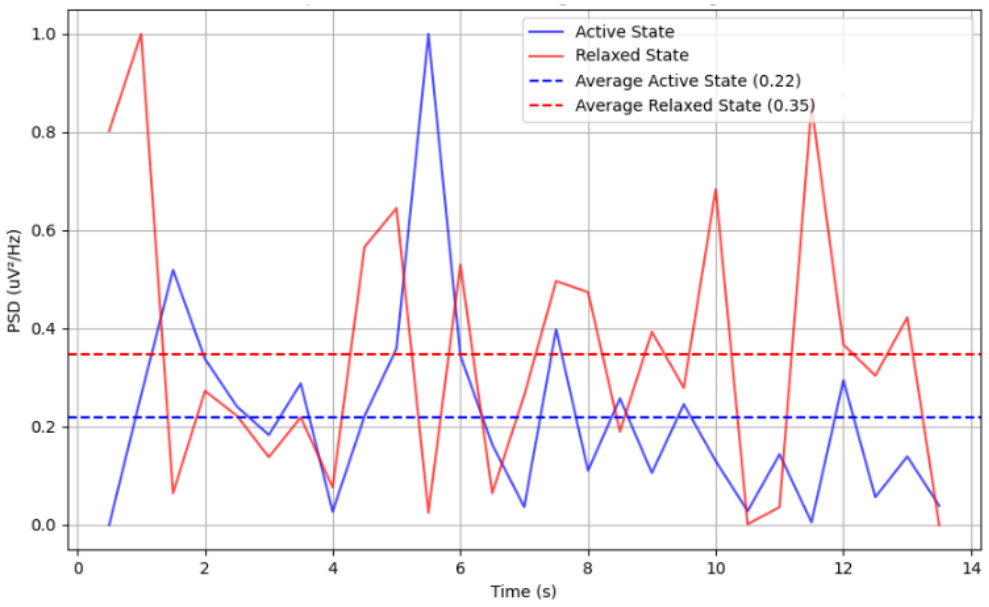


Figure 43. Healthy participants using the Emotiv headset during the experiment.

Next, Figure 44 shows the graphs obtained for Subject 4.



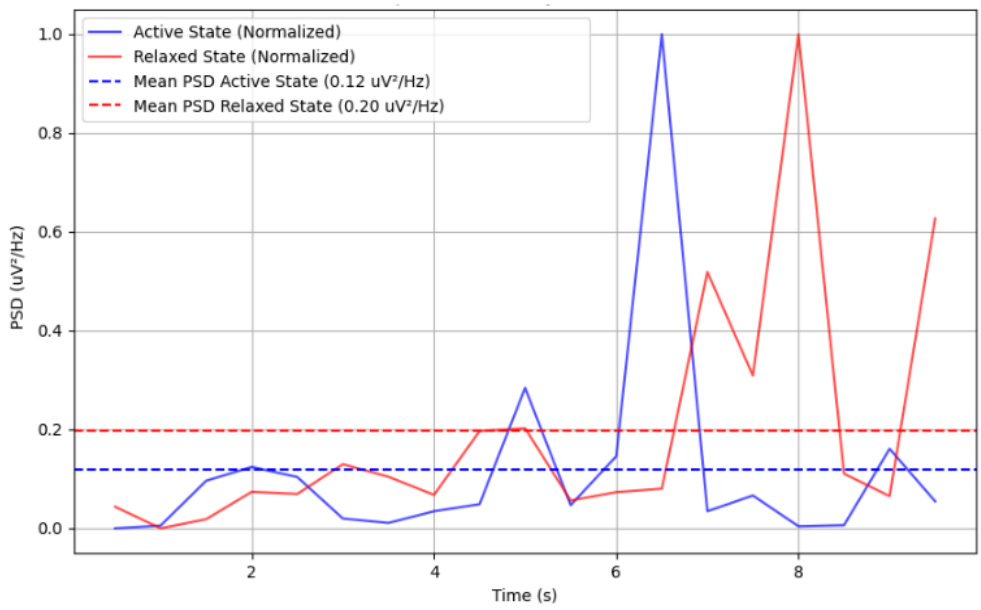
(**a**)



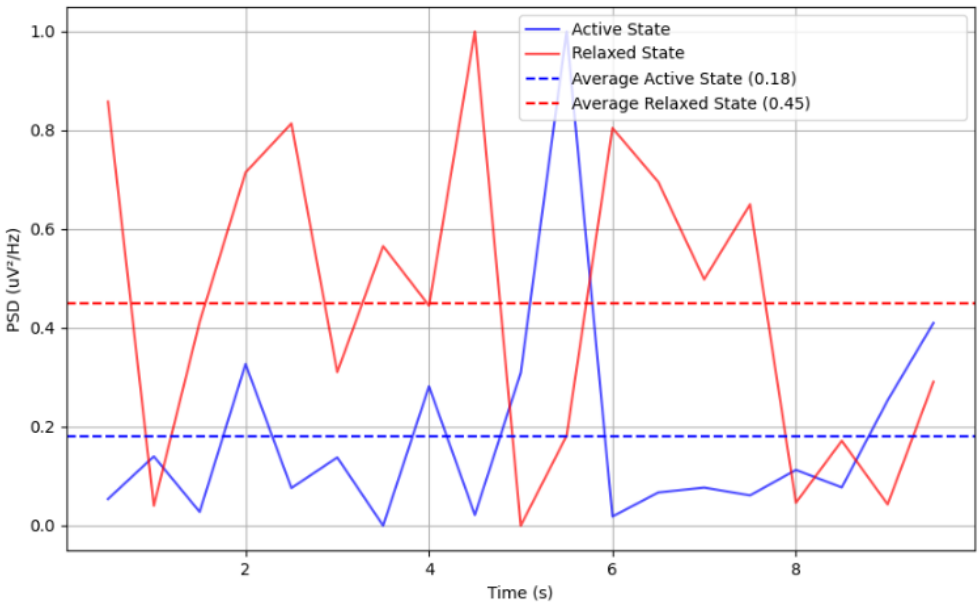
(**b**)

Figure 44. Normalized alpha PSD (8 to 13 Hz) for Subject 4 (**a**) with the Emotiv helmet, (**b**) with the Chameleon helmet.

As shown in Figure 44, the Emotiv headset had an average PSD of 0.08 $\mu V^2/Hz$ in the active state and 0.21 $\mu V^2/Hz$ in the relaxed state with a difference of 0.13 $\mu V^2/Hz$. On the other hand, the Chameleon headset recorded an average of 0.22 $\mu V^2/Hz$ in the active state and 0.35 $\mu V^2/Hz$ in the relaxed state, also obtaining a difference of 0.13 $\mu V^2/Hz$. For this case, it can be said that both headsets exhibited a quite similar behavior in differentiating between one state and the other. The results of Subject 5 are presented in Figure 45.



(**a**)



(**b**)

Figure 45. Normalized alpha PSD (8 to 13 Hz) for Subject 5 (**a**) with the Emotiv helmet, (**b**) with the Chameleon helmet.

As shown in Figure 45, the Emotiv headset had an average PSD of 0.12 $\mu V^2/Hz$ in the active state and 0.20 $\mu V^2/Hz$ in the relaxed state with a difference of 0.08 $\mu V^2/Hz$. On the other hand, the Chameleon headset recorded an average of 0.18 $\mu V^2/Hz$ in the active state and 0.45 $\mu V^2/Hz$ in the relaxed state, obtaining a difference of 0.27 $\mu V^2/Hz$. This shows a

clear difference, indicating that the Chameleon headset can better distinguish between the two states. The results of Subject 6 are presented in Figure 46.

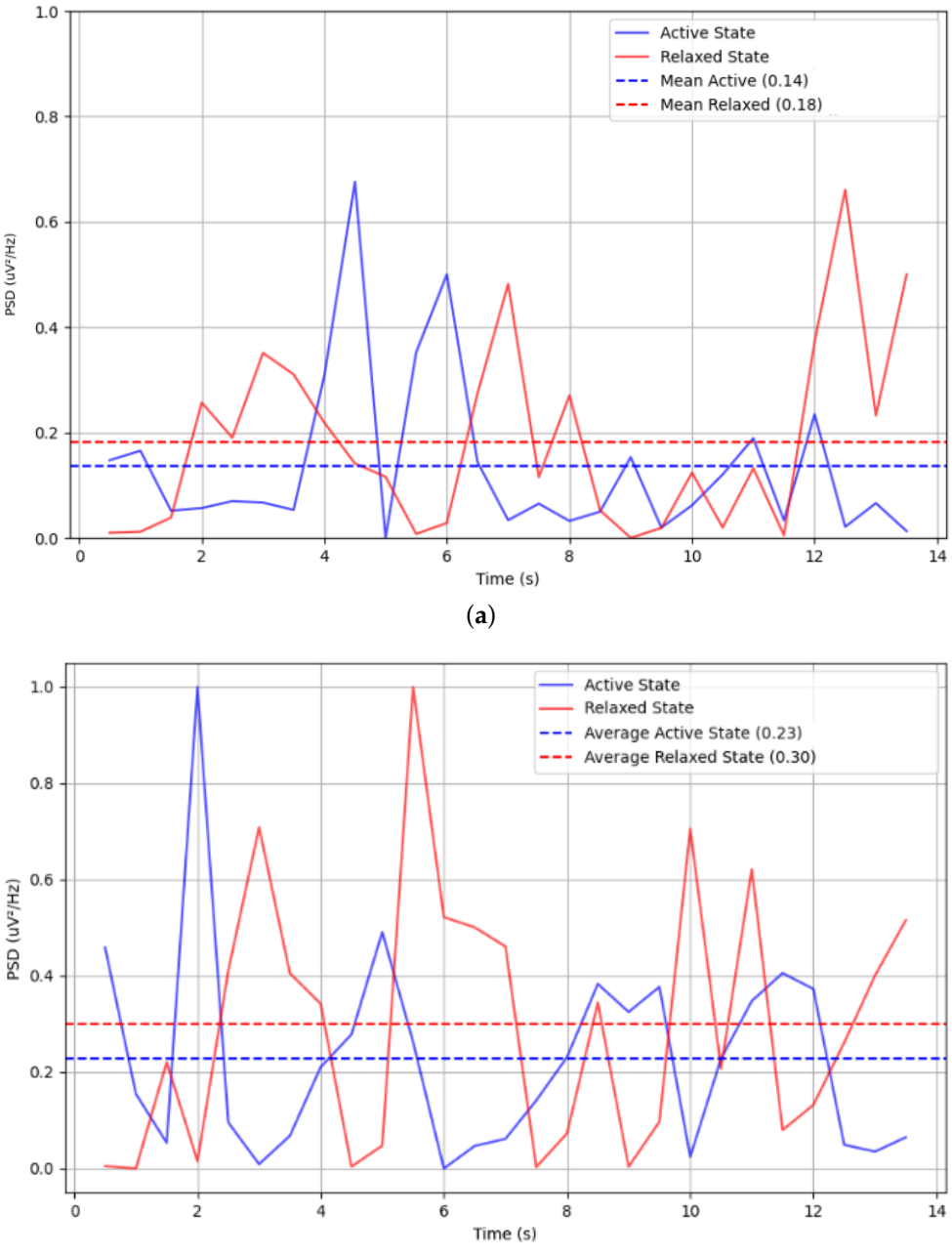


Figure 46. Normalized alpha PSD (8 to 13 Hz) for Subject 6 (**a**) with the Emotiv helmet, (**b**) with the Chameleon helmet.

As shown in Figure 46, the Emotiv headset had an average PSD of 0.14 $\mu V^2/Hz$ in the active state and 0.18 $\mu V^2/Hz$ in the relaxed state with a difference of 0.04 $\mu V^2/Hz$. On the other hand, the Chameleon headset recorded an average of 0.23 $\mu V^2/Hz$ in the active state and 0.30 $\mu V^2/Hz$ in the relaxed state, obtaining a difference of 0.07 $\mu V^2/Hz$. In this case, a small difference is observed in the measurements with the Chameleon headset showing a slightly higher value.

In Table 6, the normalized mean PSD values and standard deviations (SDs) for the different subjects are presented in both helmets.

Table 6. Comparison of normalized mean and standard deviation (SD) for power spectral density (PSD) in the 8–13 Hz range between Emotiv and Chameleon helmets.

Helmet	Subject	Mean PSD (Active State) $\mu V^2/Hz$	SD PSD (Active State) $\mu V^2/Hz$	Mean PSD (Relax State) $\mu V^2/Hz$	SD PSD (Relax State) $\mu V^2/Hz$
Emotiv	4	0.08	0.20	0.21	0.26
	5	0.12	0.22	0.20	0.24
	6	0.14	0.16	0.18	0.17
Total Mean		**0.11**	**0.19**	**0.20**	**0.22**
Chameleon	4	0.22	0.20	0.35	0.27
	5	0.18	0.22	0.45	0.31
	6	0.23	0.21	0.30	0.26
Total Mean		**0.21**	**0.21**	**0.37**	**0.28**

The results in Table 6 reveal a similar trend between both devices, which was possibly influenced by the application of normalization. In the case of the Emotiv headset, a total value of 0.11 $\mu V^2/Hz$ was obtained in the active state and 0.20 $\mu V^2/Hz$ in the relaxed state with a difference of 0.09 $\mu V^2/Hz$. However, the Chameleon recorded a total of 0.21 $\mu V^2/Hz$ in the active state and 0.37 $\mu V^2/Hz$ in the relaxed state with a difference of 0.16 $\mu V^2/Hz$. These results suggest that the Chameleon headset allowed for a slightly greater differentiation between the two states.

In general, the results showed some similarity between the Chameleon and Emotiv EPOC headsets. However, the Chameleon headset exhibited slightly better performance in distinguishing between states. It is important to note that on this occasion, normalization was applied to reduce the variability in magnitude between subjects. Although this process reduced the differences in the real magnitudes obtained between the different headsets, the contrasts between states remained perceptible.

5. Evaluation of the Technological Innovation of the Invention

In order to assess the novelty of the device, a verification was conducted to ensure that no identical or substantially similar device exists within the publicly accessible technical knowledge, thereby affirming its innovative nature. Furthermore, its distinguishing features compared to prior designs were emphasized. The primary objective of this report is to present a comprehensive analysis of prior technological developments and existing advancements in the field, providing a contextual framework for the invention within the available technical knowledge.

The databases consulted include PatFT (USPTO), Espacenet (EPO), PatentScope (WIPO), Google Patents, and SIGA (IMPI), which contain relevant information on patents, utility models, and industrial designs at both the global level and in Mexico. The invention under analysis features a design and configuration adaptable to any human skull size, enabling its use across all age groups. Moreover, it integrates manually operated mechanical mechanisms that ensure the precise positioning of each electrode at designated points on the head, thereby ensuring accurate measurements.

The technological background search conducted in the aforementioned patent databases identified eighteen patent documents deemed relevant to the present invention, as presented in Table 7.

Table 7. Results of the technological background search in patent databases.

Country/Region	Document Number	Title
Canada	CA2999152A1	Device for recording video electroencephalograms
Canada	CA3092670A1	Dynamic quantitative brain activity data collection devices, systems, and methods
China	CN115281693A	Internet-based electroencephalogram information extracting and monitoring device for pediatric neurology examination
China	CN215937398U	Adjustable electroencephalogram electrode fixing frame
China	CN216495336U	Wearable electroencephalogram detection device
China	CN216962474U	Simple and convenient electroencephalogram monitoring device
China	CN220275615U	Wearable electroencephalogram signal acquisition device
China	CN220404015U	Electroencephalogram head ring
U.S.A.	US3490439	Electrode holder for use with an electroencephalograph
U.S.A.	US3998213	Self-adjustable holder for automatically positioning electroencephalographic electrodes
U.S.A.	US7551952	EEG electrode headset
U.S.A.	US8326396	Dry electrode for detecting EEG signals and attaching device for holding the dry electrode
U.S.A.	US11701056B2	EEG measuring device
U.S.A.	US2020/178833A1	Method and system for measuring electrophysiological signals with real-time adjustment of size, electrode positioning, and spatial resolution of a headset
WIPO	WO2014/141213A1	Headset for treatment and assessment of medical conditions
WIPO	WO2017/083826A1	EEG headsets with precise and consistent electrode positioning
WIPO	WO2022/268299A1	Size-adjustable EEG headset
WIPO	WO2024/026392A2	Systems including wearable electroencephalography devices with movable band(s) and methods of use thereof

An exhaustive review of the technological landscape in scientific and technical publication databases resulted in the identification of a limited set of relevant documents, with two articles being considered especially pertinent, as detailed in Table 8.

Table 8. Summary of relevant scientific articles and documents.

Country/Region	Document Type	Ref.	Title
U.S.A.	Scientific Article	[41]	Real-time neuroimaging and cognitive monitoring using wearable dry EEG
U.S.A.	Scientific Article	[42]	Design and validation of a low-cost mobile EEG-based brain–computer interface

Finally, to complement the technological background search, an internet search was conducted using Google, identifying four websites that market brain measurement equipment, which were deemed relevant to the invention. These are presented in Table 9.

Table 9. Companies and their EEG product webpages.

Company	Website
NIHON KOHDEN	https://us.nihonkohden.com/products/vitaleeg-wireless-eeg-headset/ (accessed on 5 March 2025)
BITBRAIN TECHNOLOGIES	https://www.bitbrain.com/es/productos-neurotecnologia/dry-eeg/diadem (accessed on 5 March 2025)
ZETO INC	https://zeto-inc.com/device/ (accessed on 5 March 2025)
CGX	https://www.cgxsystems.com/quick-20m (accessed on 5 March 2025)

The search of technological background within the databases referenced in this report identified a total of eighteen patent documents, two scientific articles, and four commercial developments, all possessing technical characteristics comparable to the invention under consideration.

The analysis of the detected documents reveals that the state of the art includes various device configurations for measuring brain activity using electroencephalography (EEG) electrodes placed at strategic points on the head. Some inventions incorporate electrodes mounted on a flexible chassis made of straps, bands, or belts, allowing them to be adjusted to skulls of different sizes. Others, on the other hand, use a semi-rigid structure with flexible elements that facilitate adaptation to the user's morphology.

Some devices incorporate mechanisms to adjust the position of the electrodes, allowing precise contact with the required points on the head. One of the most common solutions involves mounting the electrodes on movable bodies that slide along the bands or straps. These movable bodies not only enable lateral adjustment but also include means to regulate the depth of the electrodes, ensuring proper contact for measurement. Other configurations position the electrodes at the ends of flexible elements, facilitating their placement without mechanical or spatial restrictions.

Although the proposed helmet incorporates some already known components, such as an adjustable chassis and mechanisms for positioning the electrodes, its design and configuration provide a solution to an unresolved problem in the state of the art: the independent adjustment of each EEG electrode's position through a mechanical mechanism in an adjustable rigid chassis.

The invention of this study comprises an adjustable chassis that includes a ring-shaped base, which is placed around the user's head, and a pair of structural arches extending from the front section of the base to its rear section. These arches incorporate slots and toothed guides that allow for modification of their dimensions to fit different skull sizes. It also features a pair of electrode positioning mechanisms, where each mechanism consists of movable links and triangular-shaped mounting bases, enabling the movement and placement of the EEG electrodes at strategic points on the head.

In light of the above and after reviewing the technical observations of prior art, we believe that the present invention presents novel and inventive aspects, according to the analyzed documents. No invention has been identified that employs a similar design and functionality for measuring brain activity to that of the proposed helmet.

6. Conclusions

The Chameleon-1 helmet has been proven in practice to exceed the initial expectations of the project, its main function being the ability to expand and adapt to any type of cranial anatomy; with this feature, it achieves great advantages compared to other similar devices. Despite its structure and the various components used, the helmet does not generate discomfort after prolonged sessions, fulfilling its objective of being ergonomic

for long periods of use. Implementing an ergonomically optimized design and improved arrangement of the electrodes allows obtaining a more precise and focused signal in the region of interest. The helmet presents good functionality, allowing for an expansion mechanism that does not compromise comfort, making it suitable for long therapy sessions. In addition, the Chameleon-1 helmet is easy to assemble and can be manipulated by anyone without the need for extensive knowledge in neurology, making it accessible and easy to use.

The findings of this study demonstrate that the Chameleon-1 helmet provides improved electrode placement precision and signal quality compared to other EEG helmets. By targeting F3 and F4, the device enables more accurate detection of brain activity states, including active and relaxed states. This improved signal reliability suggests that the helmet could be particularly useful in applications such as neurofeedback, cognitive training, and stress monitoring.

To evaluate its performance, tests were conducted on multiple subjects, monitoring theta, delta, alpha, beta, and gamma brainwave bands. The recorded signals were consistent with expected patterns based on each subject's condition, confirming the helmet's ability to capture relevant neural activity with precision. Although the Chameleon-1 helmet allows for electrode placement in additional positions within the extended 10–20 system, this study focused exclusively on the F3 and F4 locations.

Furthermore, the results show that the helmet provides consistent and reliable EEG signal detection during both concentration and relaxation phases. The enhanced electrode stability minimizes movement, leading to higher signal quality and the more precise monitoring of cognitive states.

These technological advancements reinforce the helmet's potential as a valuable tool for EEG-based research and clinical applications. However, while the study highlights its technological advantages, further research is needed to explore its full range of applications in cognitive and therapeutic settings.

The current helmet is designed to cover the frontal and frontocentral brain regions, accommodating electrodes at F3, F4, AF3, AF4, F1, F2, F5, F6, FC3, FC4, FC1, FC2, FC5, and FC6. This configuration effectively captures neural activity related to the planning and control of cognitive and motor functions. However, it does not provide full brain coverage, which may limit its applicability in studies requiring signals from other cortical areas. To address this, future developments aim to expand electrode placement to additional brain regions, enabling more comprehensive data collection and broader research applications. Another key aspect is the number of electrodes. The helmet currently features two electrodes, which are sufficient for this study's objectives. However, future iterations will focus on increasing electrode capacity and integrating advanced signal processing techniques to enhance data quality and expand the scope of applications. The use of rigid materials ensures a stable and secure fit. However, material choice can influence the weight and overall comfort. Future designs will explore more flexible and lightweight materials to improve user experience while maintaining the necessary fixation and stability.

Author Contributions: Conceptualization, A.J.H.-N. and G.O.-T.; methodology, A.F.P.-V.; software, J.-A.C.; validation, F.D.J.S.-V. and S.L.; investigation, J.Y.R.-M.; resources, N.F.D.J.; data curation, M.R.-M.; writing—original draft preparation, R.E.L.-P.; writing—review and editing, N.F.D.J.; visualization, R.I.R.-M.; supervision, J.Y.R.-M. All authors have read and agreed to the published version of the manuscript.

Funding: This research received no external funding.

Institutional Review Board Statement: The study was conducted in accordance with the Declaration of Helsinki, and was approved by the Scientific Research Ethics Committee of Centro Universitario de los Valles of the University of Guadalajara (protocol code CEI/52/2024, 7 August 2024).

Informed Consent Statement: Informed consent was obtained from all subjects involved in the study.

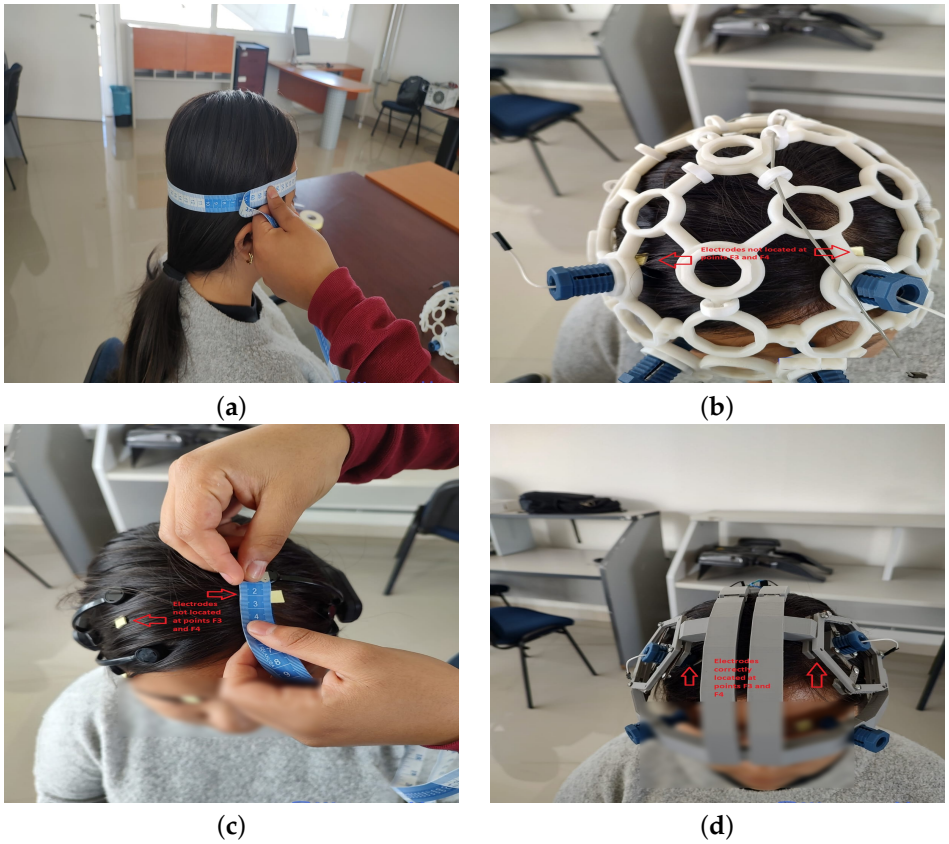
Data Availability Statement: The original contributions presented in the study are included in the article, further inquiries can be directed to the corresponding author.

Acknowledgments: We want to thank the Centro Universitario de los Valles of the University of Guadalajara for offering us the space of the artificial intelligence laboratory. This research was funded by the Jalisco State Council of Science and Technology (COECyTJAL) by the Call for Proposals of the Jalisco Scientific Development Fund to Address Social Challenges 2023 (FODECIJAL 2023) with funding number 10571-2023. Project title: CogniDron-EEG: Interfaz cerebro computadora para el entrenamiento de las funciones cognitivas.

Conflicts of Interest: The authors declare no conflicts of interest.

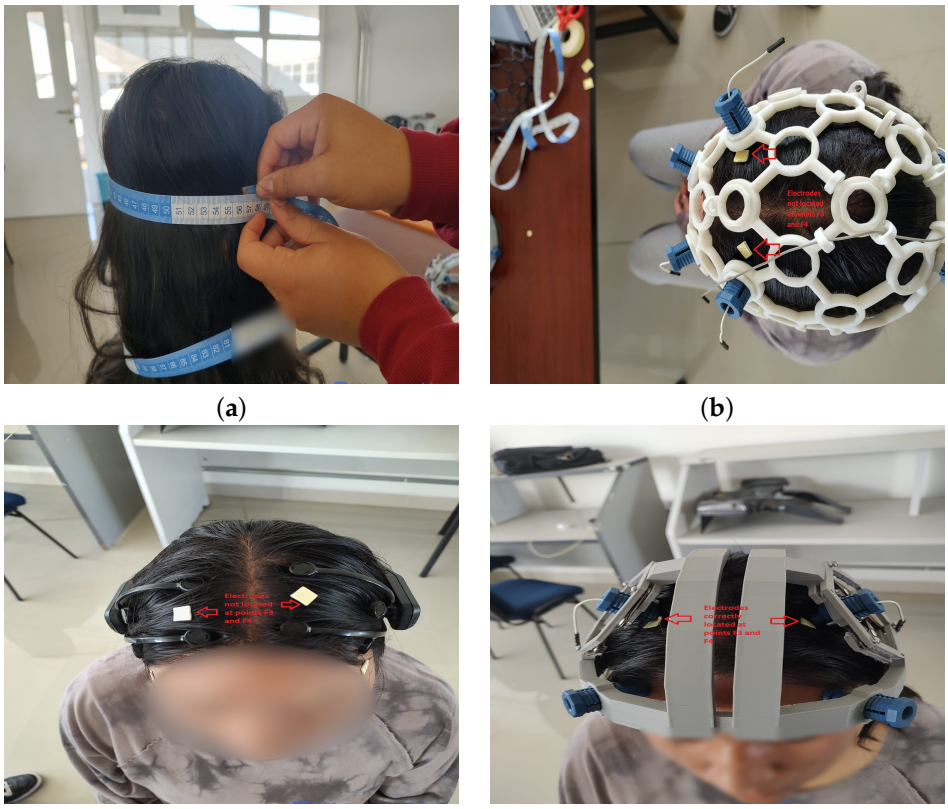
Appendix A

Point measurements (F3 and F4) and placement of the three helmets for subjects 1, 2 and 3.



(**a**) (**b**) (**c**) (**d**)

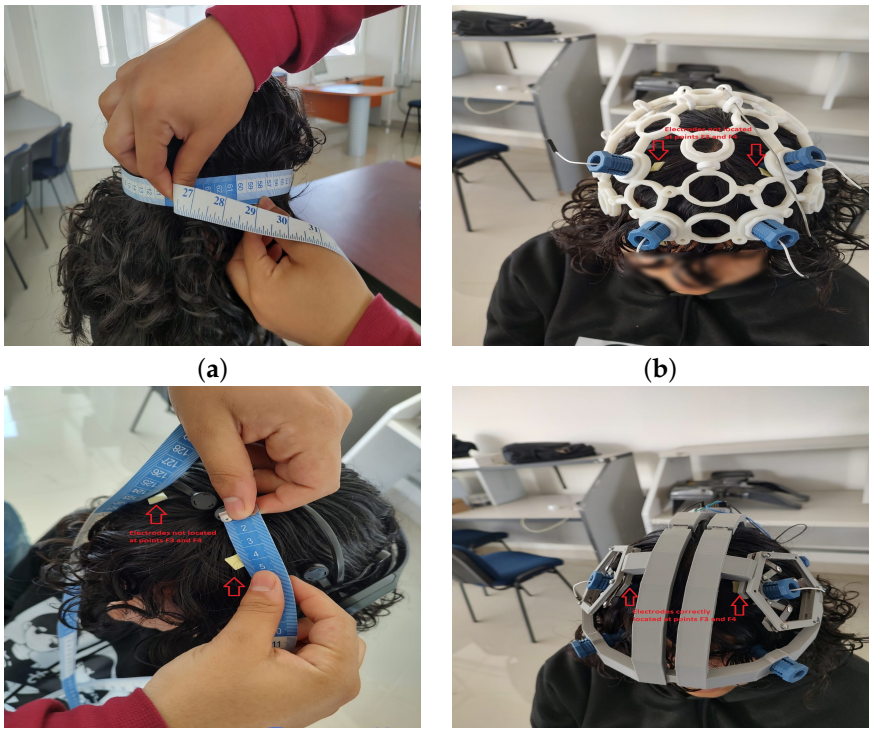
Figure A1. (**a**) Measurement of the skull of Subject 1, (**b**) position of points F3 and F4 using the Ultracortex helmet, (**c**) position and error with respect to points F3 and F4 using the Emotiv helmet, (**d**) correct position of points F3 and F4 using the Chameleon-1 helmet.



(**a**) (**b**)

(**c**) (**d**)

Figure A2. (**a**) Measurement of the skull of Subject 2, (**b**) position of points F3 and F4 using the Ultracortex helmet, (**c**) position and error with respect to points F3 and F4 using the Emotiv helmet, (**d**) correct position of points F3 and F4 using the Chameleon-1 helmet.



(**a**) (**b**)

(**c**) (**d**)

Figure A3. (**a**) Measurement of the skull of Subject 3, (**b**) position of points F3 and F4 using the Ultracortex helmet, (**c**) position and error with respect to points F3 and F4 using the Emotiv helmet, (**d**) correct position of points F3 and F4 using the Chameleon-1 helmet.

References

1. Bell, M.A.; Cuevas, K. Using EEG to study cognitive development: Issues and practices. *J. Cogn. Dev.* **2012**, *13*, 281–294. [CrossRef]
2. Jin, T.; Qi, W.; Liang, X.; Guo, H.; Liu, Q.; Xi, L. Photoacoustic Imaging of Brain Functions: Wide Filed-of-View Functional Imaging with High Spatiotemporal Resolution. *Laser Photonics Rev.* **2022**, *16*, 2100304. [CrossRef]
3. Cheng, D.; Duan, J.; Chen, H.; Wang, H.; Li, D.; Wang, Q.; Hou, Q.; Yang, T.; Hou, W.; Wang, D.; et al. Freeform OST-HMD system with large exit pupil diameter and vision correction capability. *Photon. Res.* **2022**, *10*, 21–32. [CrossRef]
4. Chang, C.; Wang, D.; Zhu, D.; Li, J.; Xia, J.; Zhang, X. Deep-learning-based computer-generated hologram from a stereo image pair. *Opt. Lett.* **2022**, *47*, 1482–1485. [CrossRef]
5. Ma, Y.; Gao, Y.; Wu, J.; Cao, L. Toward a see-through camera via AR lightguide. *Opt. Lett.* **2023**, *48*, 2809–2812. [CrossRef] [PubMed]
6. Henry, J.C. Electroencephalography: Basic principles, clinical applications, and related fields. *Neurology* **2006**, *67*, 2092–2092. [CrossRef]
7. Luck, S.J. *An Introduction to the Event-Related Potential Technique*; MIT Press: Cambridge, MA, USA, 2014.
8. Michel, C.M.; Brunet, D. EEG source imaging: A practical review of the analysis steps. *Front. Neurol.* **2019**, *10*, 325. [CrossRef]
9. Chi, Y.M.; Jung, T.P.; Cauwenberghs, G. Dry-contact and noncontact biopotential electrodes: Methodological review. *IEEE Rev. Biomed. Eng.* **2010**, *3*, 106–119. [CrossRef]
10. Casson, A.J. Wearable EEG and beyond. *Biomed. Eng. Lett.* **2019**, *9*, 53–71. [CrossRef]
11. Alchalabi, A.E.; Shirmohammadi, S.; Eddin, A.N.; Elsharnouby, M. FOCUS: Detecting ADHD Patients by an EEG-Based Serious Game. *IEEE Trans. Instrum. Meas.* **2018**, *67*, 1512–1520. [CrossRef]
12. Bleichner, M.G.; Debener, S. Concealed, unobtrusive ear-centered EEG acquisition: cEEGrids for transparent EEG. *Frontiers Hum. Neurosci.* **2017**, *11*, 163. [CrossRef] [PubMed]
13. Matthews, R.; McDonald, N.J.; Hervieux, P.; Turner, P.J.; Steindorf, M.A. A wearable physiological sensor suite for unobtrusive monitoring of physiological and cognitive state. In Proceedings of the 2007 29th Annual International Conference of the IEEE Engineering in Medicine and Biology Society, Lyon, France, 22–26 August 2007; pp. 5276–5281.
14. Oliveira, A.S.; Schlink, B.R.; Hairston, W.D.; König, P.; Ferris, D.P. Proposing metrics for benchmarking novel EEG technologies towards real-world measurements. *Front. Hum. Neurosci.* **2016**, *10*, 188. [CrossRef]
15. Hoogman, M.; Stolte, M.; Baas, M.; Kroesbergen, E. Creativity and ADHD: A review of behavioral studies, the effect of psychostimulants and neural underpinnings. *Neurosci. Biobehav. Rev.* **2020**, *119*, 66–85. [CrossRef] [PubMed]
16. Luo, Y.; Weibman, D.; Halperin, J.M.; Li, X. A review of heterogeneity in attention deficit/hyperactivity disorder (ADHD). *Front. Hum. Neurosci.* **2019**, *13*, 42. [CrossRef]
17. Cervantes, J.A.; López, S.; Cervantes, S.; Hernández, A.; Duarte, H. Social Robots and Brain—Computer Interface Video Games for Dealing with Attention Deficit Hyperactivity Disorder: A Systematic Review. *Brain Sci.* **2023**, *13*, 1172. [CrossRef] [PubMed]
18. Bul, K.C.; Franken, I.H.; Van der Oord, S.; Kato, P.M.; Danckaerts, M.; Vreeke, L.J.; Willems, A.; van Oers, H.J.; van den Heuvel, R.; van Slagmaat, R.; et al. Development and User Satisfaction of "Plan-It Commander", a Serious Game for Children with ADHD. *Games Health J.* **2015**, *4*, 502–512. [CrossRef] [PubMed]
19. Blandón, D.Z.; Muñoz, J.E.; Lopez, D.S.; Gallo, O.H. Influence of a BCI neurofeedback videogame in children with ADHD. Quantifying the brain activity through an EEG signal processing dedicated toolbox. In Proceedings of the 2016 IEEE 11th Colombian Computing Conference (CCC), Popayán, Colombia, 27–30 September 2016; pp. 1–8. [CrossRef]
20. Johnstone, S.J.; Roodenrys, S.; Johnson, K.S.; Bonfield, R.; Bennett, S.J. Game-based combined cognitive and neurofeedback training using Focus Pocus reduces symptom severity in children with diagnosed AD/HD and subclinical AD/HD. *Int. J. Psychophysiol. Off. J. Int. Organ. Psychophysiol.* **2017**, *116*, 32–44. [CrossRef]
21. Mercado, J.; Escobedo, L.; Tentori, M. A BCI video game using neurofeedback improves the attention of children with autism. *J. Multimodal User Interfaces* **2020**, *15*, 273–281. [CrossRef]
22. Cervantes, J.A.; López, S.; Molina, J.; López, F.; Tejeda, M.F.P.; Carmona-Frausto, J.C. CogniDron-EEG: A system based on a brain-computer interface and a drone for cognitive training. *Cogn. Syst. Res.* **2022**, *78*, 48–56. [CrossRef]
23. von Lühmann, A.; Kura, S.; Joseph O'Brien, W.; Zimmermann, B.B.; Duwadi, S.; Rogers, D.; Anderson, J.E.; Farzam, P.; Snow, C.; Chen, A.; et al. ninjaCap: A fully customizable and 3D printable headgear for functional near-infrared spectroscopy and electroencephalography brain imaging. *Neurophotonics* **2024**, *11*, 036601. [CrossRef]
24. Xing, L.; Casson, A.J. 3D-printed, directly conductive and flexible electrodes for personalized electroencephalography. *Sens. Actuators Phys.* **2023**, *349*, 114062. [CrossRef]
25. Kyungeun, P.; Taesuk Kihl, S.P.M.J.K.; Chang, J. Fairy tale directed game-based training system for children with ADHD using BCI and motion sensing technologies. *Behav. Inf. Technol.* **2019**, *38*, 564–577. [CrossRef]
26. Lacko, D.; Vleugels, J.; Fransen, E.; Huysmans, T.; De Bruyne, G.; Van Hulle, M.M.; Sijbers, J.; Verwulgen, S. Ergonomic design of an EEG headset using 3D anthropometry. *Appl. Ergon.* **2017**, *58*, 128–136. [CrossRef]

27. Khan, M.U.G.; Naz, Z.; Khan, J.; Saba, T.; Abunadi, I.; Rehman, A.; Tariq, U. Cognitive Skill Enhancement System Using Neuro-Feedback for ADHD Patients. *Comput. Mater. Contin.* **2021**, *68*, 2363–2376. [CrossRef]
28. Baek, H.J.; Chang, M.H.; Heo, J.; Park, K.S. Enhancing the Usability of Brain-Computer Interface Systems. *Comput. Intell. Neurosci.* **2019**, *2019*, 5427154. [CrossRef]
29. Chen, H.; Koubeissi, M.Z. Electroencephalography in Epilepsy Evaluation. *Contin. Lifelong Learn. Neurol.* **2019**, *25*, 431–453. [CrossRef]
30. Zhao, W.; Someren, E.J.V.; Li, C.; Chen, X.; Gui, W.; Tian, Y.; Liu, Y.; Lei, X. EEG spectral analysis in insomnia disorder: A systematic review and meta-analysis. *Sleep Med. Rev.* **2021**, *58*, 101457. [CrossRef]
31. Qin, Y.; Zhang, Y.; Zhang, Y.; Liu, S.; Guo, X. Application and Development of EEG Acquisition and Feedback Technology: A Review. *Biosensors* **2023**, *13*, 930. [CrossRef]
32. Hinrichs, H.; Scholz, M.; Baum, A.K.; Kam, J.W.Y.; Knight, R.T.; Heinze, H.J. Comparison between a wireless dry electrode EEG system with a conventional wired wet electrode EEG system for clinical applications. *Sci. Rep.* **2020**, *10*, 5218. [CrossRef]
33. Muhammad, R.; Ali, A.; Anwar, M.A.; Soomro, T.A.; AlShorman, O.; Alshahrani, A.; Masadeh, M.; Ashraf, G.M.; Ali, N.H.; Irfan, M.; et al. Design and Development of Low-cost Wearable Electroencephalograms (EEG) Headset. *Intell. Autom. Soft Comput.* **2023**, *35*, 26279. [CrossRef]
34. Park, S.; Han, C.H.; Im, C.H. Design of wearable EEG devices specialized for passive brain–computer interface applications. *Sensors* **2020**, *20*, 4572. [CrossRef] [PubMed]
35. Perez Vidal, A.F.; Oliver Salazar, M.A.; Salas Lopez, G. Development of a Brain-Computer Interface Based on Visual Stimuli for the Movement of a Robot Joints. *IEEE Lat. Am. Trans.* **2016**, *14*, 477–484. [CrossRef]
36. Miranda, P.; D Cox, C.; Alexander, M.; Danev, S.; RT Lakey, J. Overview of current diagnostic, prognostic, and therapeutic use of EEG and EEG-based markers of cognition, mental, and brain health. *Integr. Mol. Med.* **2019**, *6*, 378. [CrossRef]
37. Perez Vidal, A.F.; Rumbo Morales, J.Y.; Ortiz Torres, G.; Sorcia Vazquez, F.D.J.; Cruz Rojas, A.; Brizuela Mendoza, J.A.; Rodriguez Cerda, J.C. Soft exoskeletons: Development, requirements, and challenges of the last decade. *Actuators* **2021**, *10*, 166. [CrossRef]
38. You, S.D. Classification of Relaxation and Concentration Mental States with EEG. *Information* **2021**, *12*, 187. [CrossRef]
39. Vidal, A.F.P.; Cervantes, J.A.; Rumbo-Morales, J.Y.; Sorcia-Vázquez, F.D.; Ortiz-Torres, G.; Moncada, C.A.C.; Arias, I.d.l.T. Development of RelaxQuest: A Serious EEG-Controlled Game Designed to Promote Relaxation and Self-Regulation with a Potential Focus on ADHD Intervention. *Appl. Sci.* **2024**, *14*, 1173. [CrossRef]
40. Pérez-Vidal, A.F.; García-Beltrán, C.D.; Martínez-Sibaja, A.; Posada-Gómez, R. Use of the Stockwell Transform in the Detection of P300 Evoked Potentials with Low-Cost Brain Sensors. *Sensors* **2018**, *18*, 1483. [CrossRef]
41. Mullen, T.R.; Kothe, C.A.E.; Chi, Y.M.; Ojeda, A.; Kerth, T.; Makeig, S.; Jung, T.P.; Cauwenberghs, G. Real-Time Neuroimaging and Cognitive Monitoring Using Wearable Dry EEG. *IEEE Trans. Biomed. Eng.* **2015**, *62*, 2553–2567. [CrossRef]
42. Craik, A.; González-España, J.J.; Alamir, A.; Edquilang, D.; Wong, S.; Sánchez Rodríguez, L.; Feng, J.; Francisco, G.E.; Contreras-Vidal, J.L. Design and Validation of a Low-Cost Mobile EEG-Based Brain–Computer Interface. *Sensors* **2023**, *23*, 5930. [CrossRef]

Disclaimer/Publisher's Note: The statements, opinions and data contained in all publications are solely those of the individual author(s) and contributor(s) and not of MDPI and/or the editor(s). MDPI and/or the editor(s) disclaim responsibility for any injury to people or property resulting from any ideas, methods, instructions or products referred to in the content.